J|A|C|S

A R T I C L E S

A Modular Approach toward Regulating the Secondary Coordination Sphere of Metal Ions: Differential Dioxygen Activation Assisted by Intramolecular Hydrogen Bonds

Robie L. Lucas,[†] Matthew K. Zart,[†] Jhumpa Murkerjee,[†,§] Thomas N. Sorrell,[‡] Douglas R. Powell,[†] and A. S. Borovik*,[†,§]

Contribution from the Department of Chemistry, University of Kansas, 2010 Malott Hall, 1251 Wescoe Hall Drive, Lawrence, Kansas 66045, and Department of Chemistry, University of North Carolina, Chapel Hill, North Carolina 27599

Received June 5, 2006; E-mail: aborovik@uci.edu

Abstract: Metal ion function depends on the regulation of properties within the primary and second coordination spheres. An approach toward studying the structure−function relationships within the secondary coordination sphere is to construct a series of synthetic complexes having constant primary spheres but structurally tunable secondary spheres. This was accomplished through the development of hybrid urea−carboxamide ligands that provide varying intramolecular hydrogen bond (H-bond) networks proximal to a metal center. Convergent syntheses prepared ligands [(*N′-tert*-butylureayl)-*N*-ethyl]-bis(*N″*-R-carbamoyl-methyl)amine ($H_4\mathbf{1}^R$) and bis[(*N′-tert*-butylureayl)-*N*-ethyl-(*N″*-R-carbamoylmethyl)amine ($H_5\mathbf{2}^R$), where R = isopropyl, cyclopentyl, and (*S*)-(−)-α-methylbenzyl. The ligands with isopropyl groups $H_4\mathbf{1}^{iPr}$ and $H_5\mathbf{2}^{iPr}$ were combined with tris[(*N′-tert*-butylureayl)-*N*-ethyl]amine (H_6buea) and bis(*N*-isopropylcarbamoylmethyl)-amine ($H_3\mathbf{0}^{iPr}$) to prepare a series of Co(II) complexes with varying H-bond donors. $[Co^{II}H_2\mathbf{2}^{iPr}]^-$ (two H-bond donors), $[Co^{II}H\mathbf{1}^{iPr}]^-$ (one H-bond donor), and $[Co^{II}\mathbf{0}^{iPr}]^-$ (no H-bond donors) have trigonal monopyramidal primary coordination spheres as determined by X-ray diffraction methods. In addition, these complexes have nearly identical optical and EPR properties that are consistent with $S = \frac{3}{2}$ ground states. Electrochemical studies show a linear spread of 0.23 V in anodic potentials (E_{pa}) with $[Co^{II}H_2\mathbf{2}^{iPr}]^-$ being the most negative at −0.385 V vs $[Cp_2Fe]^+/[Cp_2Fe]$. The properties of $[Co^{II}H_3buea]^-$ (H_3buea, tris[(*N′-tert*-butylureaylato)-*N*-ethyl]aminato that has three H-bond donors) appears to be similar to that of the other complexes based on spectroscopic data. $[Co^{II}H_3buea]^-$ and $[Co^{II}H_2\mathbf{2}^{iPr}]^-$ react with 0.5 equiv of dioxygen to afford $[Co^{III}H_3buea(OH)]^-$ and $[Co^{III}H_2\mathbf{2}^{iPr}(OH)]^-$. Isotopic labeling studies confirm that dioxygen is the source of the oxygen atom in the hydroxo ligands: $[Co^{III}H_3buea(^{16}OH)]^-$ has a $\nu(O-H)$ band at 3589 cm^{-1} that shifts to 3579 cm^{-1} in $[Co^{III}H_3buea(^{18}OH)]^-$; $[Co^{III}H_2\mathbf{2}^{iPr}(OH)]^-$ has $\nu(^{16}O-H)$ = 3661 and $\nu(^{18}O-H)$ = 3650 cm^{-1}. $[Co^{II}H\mathbf{1}^{iPr}]^-$ does not react with 0.5 equiv of O_2; however, treating $[Co^{II}H\mathbf{1}^{iPr}]^-$ with excess dioxygen initially produces a species with an X-band EPR signal at $g = 2.0$ that is assigned to a Co−O$_2$ adduct, which is not stable and converts to a species having properties similar to those of the Co^{III}−OH complexes. Isolation of this hydroxo complex in pure form was complicated by its instability in solution ($k_{int} = 2.5 \times 10^{-7}$ M min^{-1}). Moreover, the stability of the Co^{III}−OH complexes is correlated with the number of H-bond donors within the secondary coordination sphere; $[Co^{III}H_3buea(OH)]^-$ is stable in solution for days, whereas $[Co^{III}H_2\mathbf{2}^{iPr}(OH)]^-$ decays with a $k_{int} = 5.9 \times 10^{-8}$ M min^{-1}. The system without any intramolecular H-bond donors $[Co^{II}\mathbf{0}^{iPr}]^-$ does not react with dioxygen, even when O_2 is in excess. These findings indicate a correlation between dioxygen binding/activation and the number of H-bond donors within the secondary coordination sphere of the cobalt complexes. Moreover, the properties of the secondary coordination sphere affect the stability of the Co^{III}−OH complexes with $[Co^{III}H_3buea(OH)]^-$ being the most stable. We suggest that the greater number of intramolecular H-bonds involving the hydroxo ligand reduces the nucleophilicity of the Co^{III}−OH unit and reinforces the cavity structure, producing a more constrained microenvironment around the cobalt ion.

Introduction

Transition metal complexes are used in a variety of applications, including as reagents for chemical synthesis.[1] This interest

has led to the development of multidentate ligands that aid in controlling the chemistry at the metal center. Many of these ligands are designed to influence the primary coordination

---

[†] University of Kansas.
[‡] University of North Carolina.
[§] Current address: Department of Chemistry, University of California, Irvine, CA 92697.

(1) For selected recent reviews: (a) Nakamura, I.; Yamamoto, Y. *Chem. Rev.* **2004**, *104*, 2127−2198. (b) Trost, B. M.; Crawley, M. L. *Chem. Rev.* **2003**, *103*, 2921−2943. (c) Uma, R.; Crévisy, C.; Grée, R. *Chem. Rev.* **2003**, *103*, 27−51. (d) *Transition Metals for Organic Synthesis*, 2nd ed.; Beller, M., Bolm, C., Eds.; Wiley-CH: Weinheim, Germany, 2004; Vol. 1−2.
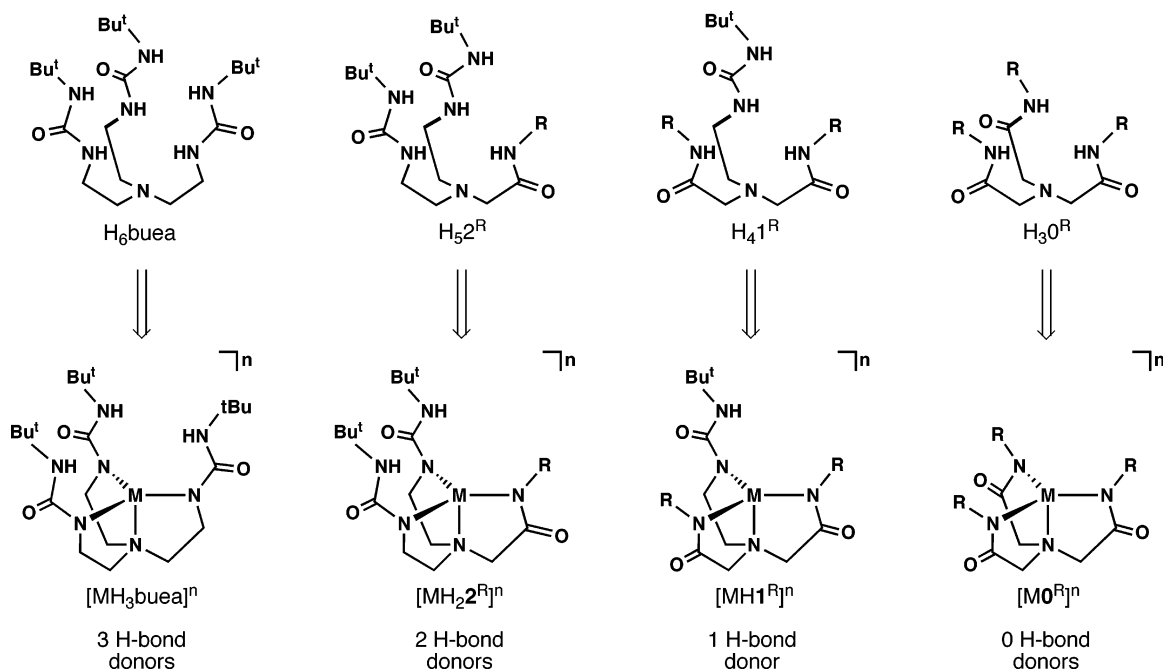
Figure 1. Series of ligands and complexes having varied intramolecular H-bond networks.

sphere of a metal complex, which ultimately affects properties related to electronic structure and acidity.[2] While often overlooked, the secondary coordination sphere also can have a crucial role in determining the functional properties of metal complexes. In fact, it is becoming increasingly apparent that managing both spheres around a metal ion is necessary to achieve desirable functions.

Placing hydrogen bond (H-bond) donors and acceptors proximal to a metal center is one approach for controlling the secondary coordination sphere. The key impetus for this approach comes from structural studies on metalloproteins that show active site architectures with H-bonds involving ligands coordinated to the metal ion(s).[3] These noncovalent interactions assist in modulating structural features around the active metal center(s) that, in turn, help regulate protein function. Transferring these structure−function relationships to synthetic systems is often difficult because H-bonds tend to form intermolecularly with other species in the reaction milieu; the sought after *intramolecular* interactions are usually obtainable only when the H-bond donors/acceptors are tethered to a rigid framework. Nevertheless, there are now examples of systems that form intramolecular H-bonds to exogenous ligands, most often in studies aimed at molecular recognition processes.[4]

Our group[5] and others[6] have used tripodal ligands as a means to position H-bond donors or acceptors near metal centers. We have developed urea-based tripods that create a rigid H-bonding cavity around vacant coordination sites when the ligand binds to a metal ion. For instance, the symmetrical ligand tris[(N′-tert-butylureaylato)-N-ethyl]aminato ([H_3buea]$^{3-}$) places three H-bond donors within the interior of a cavity adjacent to a coordinated metal ion (Figure 1). We have shown that iron(II) and manganese(II) complexes of [H_3buea]$^{3-}$ bind and activate dioxygen to form M^{III}−O complexes in which three intramolecular H-bonds are formed with the terminal oxo ligand.

Complexes of [H_3buea]$^{3-}$ contain a fixed number of H-bonds within the secondary coordination sphere, producing a relatively constant H-bond network; in fact, most reported systems to date have a set amount of H-bond donors/acceptors. To fully understand the effects of H-bonds on metal-mediated processes, it is necessary to know how *varying* H-bond networks correlate with changes in function. An approach to probe these structure−function correlations requires the development of structurally tunable cavities, which can be accomplished through the design and preparation of ligands that provide similar primary coordination spheres but different architectures and noncovalent interactions in the secondary coordination sphere. Few systems

(2) Constable, E. C. *Metals and Ligand Reactivity*; VCH: Weinheim, Germany, 1996.

(3) (a) Lu, Y.; Valentine, J. S. *Curr. Opin. Struct. Biol.* **1997**, *7*, 495−500. (b) Regan, L. *TIBS* **1995**, *20*, 280−285.

(4) Selected relevant examples: (a) Jameson, G. B.; Drago, R. S. *J. Am. Chem. Soc.* **1985**, *107*, 3017−3020. (b) Momenteau, M.; Reed, C. A. *Chem. Rev.* **1994**, *94*, 659−698. (c) Collman, J. P. *Inorg. Chem.* **1997**, *36*, 5145−5155. (d) Collman, J. P.; Zhang, X.; Wong, K.; Brauman, J. *J. Am. Chem. Soc.* **1994**, *116*, 6245−6251. (e) Wuenschell, G. E.; Tetreau, C.; Lavalette, D.; Reed, C. A. *J. Am. Chem. Soc.* **1992**, *114*, 3346−3355. (f) Chang, C. K.; Liang, Y.; Avilés, G. *J. Am. Chem. Soc.* **1995**, *117*, 4191−4192. (g) Yeh, C.-Y.; Chang, C. J.; Nocera, D. G. *J. Am. Chem. Soc.* **2001**, *123*, 1513−1514. (h) Rudkevich, D. M.; Verboom, W.; Brzozka, Z.; Palys, M. J.; Stauthamer, W. P. R. V.; Van Hummel, G. J.; Franken, S. M.; Harkema, S.; Engbersen, J. F. J.; Reinhoudt, D. N *J. Am. Chem. Soc.* **1994**, *116*, 4341−4351. (i) Kickham, J. E.; Loeb, S, L.; Murphy, S. L. *J. Am. Chem. Soc.* **1993**, *115*, 7031−7032. (j) Walton, P. H.; Raymond, K. N. *Inorg. Chim. Acta* **1995**, *240*, 593−601.

(5) (a) Hammes, B. S.; Young, V. G., Jr.; Borovik, A. S. *Angew. Chem., Int. Ed.* **1999**, *38*, 666−669. (b) Shirin, Z.; Hammes, B. S.; Young, V. G., Jr.; Borovik, A. S. *J. Am. Chem. Soc.* **2000**, *122*, 1836−1837. (c) MacBeth, C. E.; Golombek, A. P.; Young, V. G., Jr.; Yang, C.; Kuczera, K.; Hendrich, M. P.; Borovik, A. S. *Science* **2000**, *289*, 938−941. (d) MacBeth, C. E.; Hammes, B. S.; Young, V. G., Jr.; Borovik, A. S. *Inorg. Chem.* **2001**, *40*, 4733−4741. (e) Gupta, R. G.; MacBeth, C. E.; Young, V. G., Jr.; Borovik, A. S. *J. Am. Chem. Soc.* **2002**, *124*, 1136−1137. (f) Gupta, R.; Borovik, A. S. *J. Am. Chem. Soc.* **2003**, *125*, 13234−13242. (g) Zart, M. K.; Sorrell, T. N.; Powell, D.; Borovik, A. S. *J. Chem. Soc., Dalton Trans.* **2003**, 1986−1992. (h) MacBeth, C. E.; Gupta, R.; Mitchell-Koch, K. M.; Young, V. G., Jr.; Lushington, G. H.; Thompson, W. H.; Hendrich, M. P.; Borovik, A. S. *J. Am. Chem. Soc.* **2004**, *126*, 2556−2567. (i) Larsen, P. L.; Gupta, R.; Powell, D. R.; Borovik, A. S. *J. Am. Chem. Soc.* **2004**, *126*, 6622−6623. (j) Borovik, A. S. *Acc. Chem. Res.* **2005**, *38*, 54−61. (k) Lucas, R. L.; Powell, D. R.; Borovik, A. S. *J. Am. Chem. Soc.* **2005**, *127*, 11597−11598. (l) Zinn, P. J.; Powell, D. R.; Hendrich, M. P.; Sorrell, T. N.; Borovik, A. S. *Inorg. Chem.* **2006**, *45*, 3484−3486.

have been reported with these attributes, the closest examples being those involving polypyridine ligands having various numbers of amino groups available for hydrogen bonding.[7,8] Masuda has used these ligands to prepare a series of Cu[II]−azide complexes: spectroscopic and structural characterization indicated that as the number of amino groups on the tripodal ligands increased, the geometry around the Cu(II) ion changed from ideal trigonal bipyramidal to a geometry between trigonal bipyramidal and square pyramidal.[7] The change in coordination geometry was attributed to increased steric repulsion between the amino groups and the coordinated azide ion bonded to the Cu(II) ion. In a separate study, Mareque-Rivas probed the effects of H-bonds on the acidity of Zn(II)−water complexes;[8a,b] the placement of two H-bond donors proximal to the Zn(II)-bound water molecule enhances its acidity nearly 2 orders of magnitude.

The limited number of transition metal complexes with varied H-bond networks is directly linked to the paucity of ligands that produce a constant primary coordination sphere while conveniently allowing systematic adjustments to the secondary coordination sphere. We have therefore developed tripodal urea−carboxamide hybrid ligands that are prepared via straightforward convergent syntheses. The ligands[9,10] $H_5\mathbf{2}^R$ and $H_4\mathbf{1}^R$ (Figure 1) contain at least one urea arm and, together with H_6-buea and $H_3\mathbf{0}^R$,[11] constitute a series of ligands whose metal complexes have equivalent primary coordination spheres but different H-bond networks within the secondary coordination sphere. The assessment of structure−function relationships is illustrated with a series of Co(II) complexes having similar coordination geometries and spectroscopic properties but differing in their abilities to bind and activate dioxygen.

(6) (a) Harata, M.; Jitsukawa, K.; Masuda, H.; Einaga, H. *Chem. Lett.* **1995**, 61−62. (b) Ogo, S.; Wada, S.; Watanabe, Y.; Iwase, M.; Wada, A.; Harata, M.; Jitsukawa, K.; Masuda, H.; Einaga, H. *Angew. Chem., Int. Ed.* **1998**, *37*, 2102−2104. (c) Berreau, L. M.; Allred, R. A.; Makowska-Grzyska, M.; Arif, A. M. *Chem. Commun.* **2000**, 1423−1424. (d) Berreau, L. M.; Makowska-Grzyska, M. M.; Arif, A. M. *Inorg. Chem.* **2001**, *40*, 2212−2213. (e) Garner, D. K.; Fitch, S. B.; McAlexander, L. H.; Bezold, L. M.; Arif, A. M.; Berreau, L. M. *J. Am. Chem. Soc.* **2002**, *124*, 9970−9971. (f) Ogo, S.; Yamahara, R.; Roach, M.; Suenobu, T.; Aki, M.; Ogura, T.; Kitagawa, T.; Masuda, H.; Fukuzumi, S.; Watanabe, Y. *Inorg. Chem.* **2002**, *41*, 5513−5520. (g) Cheruzel, L. E.; Wang, J.; Mashuta, M. S.; Buchanan, R. M. *Chem. Commun.* **2002**, 2166−2167. (h) Tubbs, K. J.; Fuller, A. L.; Bennett, B.; Arif, A. M.; Berreau, L. M. *Inorg. Chem.* **2003**, *42*, 4790−4791. (i) Mareque-Rivas, J. C.; Torres Martín de Rosales, R.; Parsons, S. *Dalton Trans.* **2003**, 2156−2163. (j) Mareque-Rivas, J. C.; Torres Martín de Rosales, R.; Parsons, S. *Chem. Commun.* **2004**, 610−611. (k) Mareque-Rivas, J. C.; Salvagni, E.; Parsons, S. *Chem. Commun.* **2004**, 460−461. (l) Mareque-Rivas, J. C.; Salvagni, E.; Parsons, S. *Dalton Trans.* **2004**, 4185−4192. (m) Cheruzel, L. E.; Cecil, M. R.; Edison, S. E.; Mashuta, M. S.; Baldwin, M. J.; Buchanan, R. M. *Inorg. Chem.* **2006**, *45*, 3191−3202.

(7) Wada, A.; Honda, Y.; Yamaguchi, S.; Nagatomo, S.; Kitagawa, T.; Jitsukawa, K. *Inorg. Chem.* **2004**, *43*, 5725−5735.

(8) (a) Mareque-Rivas, J. C.; Prabaharan, R.; Torres Martín de Rosales, R. *Chem. Commun.* **2004**, 76−77. (b) Mareque-Rivas, J. C.; Prabaharan, R.; Parsons, S. *Dalton Trans.* **2004**, 1648−1655. (c) Mareque-Rivas, J. C.; Salvagni, E.; Parsons, S. *Dalton Trans.* **2004**, 4185−4192.

(9) The bold numbers in the abbreviations for the hybrid ligands denote the number of H-bond donating groups; $H_4\mathbf{1}^R$ and $H_5\mathbf{2}^R$ have one and two H-bond donors, respectively. The ligands containing only amide groups, $H_3\mathbf{0}^R$ has no H-bond donors and is thus indicated by the zero. The ligand with three urea groups, H₆buea has been reported previously and its name is unchanged for consistency.

(10) A report containing these ligands in iron-amido chemistry has recently appeared: Lucas, R. L.; Powell, D. R.; Borovik, A. S. *J. Am. Chem. Soc.* **2005**, *127*, 11597−11598.

(11) (a) Ray, M.; Yap, G. P. A.; Rheingold, A. L.; Borovik, A. S. *Chem. Commun.* **1995**, 1977−1978. (b) Ray, M.; Golombek, A. P.; Hendrich, M. P.; Young, V. G., Jr.; Borovik, A. S. *J. Am. Chem. Soc.* **1996**, *118*, 6084−6085. (c) Ray, M.; Golombek, A. P.; Hendrich, M. P.; Yap, G. P. A.; Liable-Sands, L. M.; Rheingold, A. L.; Borovik, A. S. *Inorg. Chem.* **1999**, *38*, 3110−3115. (d) Ray, M.; Hammes, B. S.; Yap, G. P. A.; Rheingold, A. L.; Borovik, A. S. *Inorg. Chem.* **1998**, *37*, 1527−1532. (e) Shirin, Z.; Young, V. G.; Borovik, A. S. *Chem. Commun.* **1997**, *4*, 1967−1968. (f) Hammes, B. S.; Maldonado-Ramos, D.; Yap, G. P. A.; Liable-Sands, L.; Rheingold, A. L.; Borovik, A. S. *Inorg. Chem.* **1997**, *36*, 3210−3211.

Experimental Section

General Methods. All reagents were purchased from commercial sources and used as received, unless otherwise noted. Solvents were purified according to standard procedures. Anhydrous solvents were purchased from Aldrich. Potassium hydride (KH) as a 30% dispersion in mineral oil was filtered with a medium porosity glass frit and washed 5 times each with pentane and Et₂O. The solid KH was dried under a vacuum and stored under an inert atmosphere. The syntheses of ligands and their intermediates were carried out under a dinitrogen atmosphere. The syntheses of metal complexes were conducted in a Vacuum Atmospheres, Co. drybox under an argon atmosphere. Dioxygen was dried on a Drierite gas purifier purchased from Fischer Scientific. ¹⁸O₂ was obtained from ICON Isotopes (Summit, NJ). Elemental analyses were accomplished at Desert Analytics, Tucson, AZ. The preparations of H₃0 and H₆buea have been published previously.[5b,11b] The synthesis of [Co[III]H₃buea(OH)]⁻ using water as the source of hydroxide has also been reported.[5a]

Preparative Methods. 1-*tert*-Butyl-3-(2-chloroethyl)urea (3) To a suspension of 2-chloroethylamine hydrochloride (11.54 g, 99.49 mmol) in 100 mL of THF was added NaHCO₃ (9.20 g, 110 mmol). The mixture was treated dropwise with *tert*-butyl isocyanate (12.5 mL, 109 mmol) and allowed to stir overnight. The mixture was then filtered, and the white solid was washed with THF. The colorless filtrate was concentrated under reduced pressure to a white solid, which was recrystallized from Et₂O and dried under a vacuum to 14.5 g (81%). Mp 99−101 °C; ¹H NMR (400 MHz, DMSO-d_6) δ 5.93 (1H, t, J = 6.0 Hz, CH₂N*H*), 5.85 (1H, s, N*H*−C(CH₃)₃), 3.55 (2H, t, J = 6.0 Hz, CH₂C*H₂*Cl), 3.27 (2H, dt, J = 6.0 Hz, NH−C*H₂*CH₂), 1.21 (9H, s, C(C*H₃*)₃); ¹³C NMR (500 MHz, CDCl₃) δ 157.7, 50.1, 44.7, 41.7, 29.5; FTIR (Nujol) 3367 (N−H), 3348 (N−H), 1632 (C=O); HRMS (ES+): Exact mass calcd for C₇H₁₆N₂OCl [M + H], 179.0951. Found 179.0958.

1-*tert*-Butyl-3-(2-phthalimidooethyl)urea (4). A solution of chloride **3** (14.38 g, 80.49 mmol) in 80 mL of anhydrous DMF was treated with potassium phthalimide (29.82 g, 161.0 mmol), and the resulting mixture was heated at 120 °C for 3 h with stirring. The pale pink mixture was brought to rt and then poured into 400 mL of H₂O to produce a white precipitate, which was filtered, washed with H₂O, and dried overnight under a vacuum at 70 °C. The white solid was recrystallized from acetone/hexanes and dried under a vacuum to 17.04 g (73%). Mp 199−200 °C; ¹H NMR (400 MHz, DMSO-d_6) δ 7.83 (4H, m, Ar*H*), 5.73 (1H, t, J = 6.0 Hz, CH₂N*H*), 5.55 (1H, s, N*H*-C(CH₃)₃), 3.57 (2H, t, J = 5.7 Hz, CH₂C*H₂*NPhth), 3.23 (2H, dt, J = 5.7, 6.0 Hz, NH−C*H₂*CH₂), 1.06 (9H, s, C(C*H₃*)₃); ¹³C NMR (500 MHz, CDCl₃) δ 168.6, 157.1, 134.0, 132.0, 123.3, 50.4, 39.3, 38.3, 29.3; FTIR (KBr) 3364 (N−H), 3340 (N−H), 1720 (imide C=O), 1709 (imide C=O), 1631 (urea C=O); HRMS (FAB+): Exact mass calcd for C₁₅H₂₀N₃O₃ [M + H], 290.1505. Found 290.1505.

1-(2-Aminoethyl)-3-*tert*-butylurea (5). A suspension of phthalimide **4** (10.75 g, 37.15 mmol) in 375 mL of EtOH was treated with hydrazine monohydrate (9.30 g, 186 mmol) and heated to reflux, resulting in a homogeneous solution. Over the course of refluxing for 3 h a voluminous white ppt (phthalhydrazide) formed. The mixture was cooled to rt, and the precipitate was filtered and washed with EtOH. The colorless filtrate was concentrated under reduced pressure to an oil, which was treated with 95 mL of CHCl₃, resulting in precipitation of more phthalhydrazide. The ppt was filtered and washed with CHCl₃. The filtrate was concentrated to an oil and dried under a vacuum to a white solid weighing 5.92 g (100%). ¹H NMR (500 MHz, DMSO-d_6) δ 5.69 (1H, t, J = 5.6 Hz, CH₂N*H*), 5.67 (1H, s, N*H*−C(CH₃)₃), 2.93 (2H, dt, J = 5.6, 6.2 Hz, NH−C*H₂*CH₂), 2.51 (2H, t, J = 6.2 Hz, CH₂C*H₂*-NH₂), 1.21 (9H, s, C(C*H₃*)₃); ¹³C NMR (500 MHz, DMSO-d_6) δ 157.9, 49.3, 42.7, 42.5, 29.7; FTIR (thin film from CH₂Cl₂) 3350 (N−H), 1645 (C=O); HRMS (FAB+): Exact mass calcd for C₇H₁₈N₃O [M + H], 160.1450. Found 160.1469.

Bis[(N′-tert-butylureayl)-N-ethyl]benzylamine (6). A mixture of benzylamine (6.11 g, 57.0 mmol), chloride **3** (21.38 g, 119.7 mmol), Et$_3$N (13.3 g, 131 mmol), and NaI (85 mg, 0.57 mmol) in 250 mL of THF was refluxed for 48 h. The mixture was cooled to rt, and Et$_3$N· HCl that precipitated from the reaction mixture was removed by filtration. The filtrate was concentrated under reduced pressure to an orange oil that solidified upon standing overnight. The solid was triturated with EtOAc to produce a white solid that was filtered, washed with EtOAc followed by Et$_2$O, and dried under a vacuum to 15.18 g. The filtrate from the trituration was concentrated to an orange oil and then eluted through a plug of silica gel with EtOAc. The pale yellow solid obtained was filtered and washed with Et$_2$O to give a white solid. The solid was dried under a vacuum to 1.90 g, giving a combined yield of 17.08 g (77%). Mp 173−175 °C; ^{1}H NMR (400 MHz, DMSO-d_6) δ 7.34−7.22 (5H, m, Ar*H*), 5.75 (2H, t, J = 5.7 Hz, CH$_2$N*H*), 5.71 (2H, s, N*H*—C(CH$_3$)$_3$), 3.57 (2H, s, C*H*$_2$Ph), 3.03 (4H, dt, J = 5.7, 6.0 Hz, NH—C*H*$_2$CH$_2$), 2.39 (4H, t, J = 6.0 Hz, CH$_2$C*H*$_2$NBn), 1.23 (18H, s, C(C*H*$_3$)$_3$); ^{13}C NMR (500 MHz, CDCl$_3$) δ 158.5, 139.7, 129.0, 127.9, 126.8, 59.3, 55.6, 49.9, 37.8, 29.6; FTIR (KBr) 3377 (N—H), 3274 (N—H), 1632 (C=O); HRMS (FAB+): Exact mass calcd for C$_{21}$H$_{38}$N$_5$O$_2$ [M + H], 392.3026. Found 392.3033.

Bis[(N′-tert-butylureayl)-N-ethyl]amine (7). To a solution of **6** (7.86 g, 20.1 mmol) in 150 mL of MeOH and 75 mL of cyclohexene was added 10% Pd/C (750 mg). The suspension refluxed for 4 h. After cooling to rt the mixture was filtered through a pad of Celite. The filtrate was concentrated under reduced pressure, and the residue was treated with Et$_2$O to produce a white solid. The white solid was filtered, washed with Et$_2$O, and dried under a vacuum to 5.19 g (86%). Mp 177−179 °C; ^{1}H NMR (400 MHz, DMSO-d_6) δ 5.68 (2H, s, N*H*—C(CH$_3$)$_3$), 5.65 (2H, t, J = 5.7 Hz, CH$_2$N*H*—CO), 2.99 (4H, dt, J = 5.7, 6.3 Hz, CO—NH—C*H*$_2$CH$_2$), 2.48 (4H, t, J = 6.3 Hz, CH$_2$C*H*$_2$NH—C*H*$_2$), 1.20 (18H, s, C(C*H*$_3$)$_3$); ^{13}C NMR (500 MHz, CDCl$_3$) δ 158.2, 50.3, 49.3, 40.0, 29.6; FTIR (KBr) 3358 (N—H), 3324 (N—H), 1635 (C=O); HRMS (ES+): Exact mass calcd for C$_{14}$H$_{32}$N$_5$O$_2$ [M + H], 302.2556. Found 302.2554.

N-Isopropyl-2-bromoacetamide (8). A solution of isopropylamine (19.69 g, 333.1 mmol) dissolved in 350 mL of CH$_2$Cl$_2$ was cooled to 0 °C with an ice water bath. Bromoacetyl bromide (33.61 g, 166.5 mmol) was added to the solution dropwise over 15 min, during which time a white ppt formed. The mixture was warmed to rt and stirred for 1 h, and the white ppt was filtered and washed with CH$_2$Cl$_2$. The colorless filtrate was washed with 2 M HCl (1 × 175 mL) and brine (1 × 175 mL). The solution was dried over Na$_2$SO$_4$, filtered, and concentrated under reduced pressure to a white solid, which was dried under a vacuum to 25.60 g (85%). Mp 63−64 °C (lit.[12] 66−67 °C); ^{1}H NMR (400 MHz, CDCl$_3$) δ 6.32 (1H, bs, N*H*), 4.05 (1H, m, NH—C*H*(CH$_3$)$_2$), 3.84 (2H, s, BrC*H*$_2$), 1.18 (6H, d, J = 6.6 Hz, CH(C*H*$_3$)$_2$); ^{13}C NMR (400 MHz, CDCl$_3$) δ 164.4, 42.3, 29.4, 22.4; FTIR (thin film from CH$_2$Cl$_2$) 3285 (N—H), 1644 (C=O); LRMS (FAB+): Found for C$_5$H$_{11}$BrNO [M + H], 180.1.

N-Cyclopentyl-2-bromoacetamide (9). Following a similar protocol used for the preparation of **8**, reaction between cyclopentylamine (13.53 g, 158.9 mmol) and bromoacetyl bromide (16.0 g, 79.3 mmol) gave 14.21 g (87%) of compound **9** as a white solid. Mp 84−85 °C; ^{1}H NMR (400 MHz, CDCl$_3$) δ 6.44 (1H, bs, N*H*), 4.19 (1H, m, NH—C*H*), 3.87 (2H, s, BrC*H*$_2$), 2.01 (2H, m, cypC*H*$_2$), 1.70 (2H, m, cypC*H*$_2$), 1.63 (2H, m, cypC*H*$_2$), 1.43 (2H, m, cypC*H*$_2$); ^{13}C NMR (400 MHz, CDCl$_3$) δ 164.8, 51.8, 32.8, 29.4, 23.6; FTIR (KBr) 3281 (N—H), 1647 (C=O); HRMS (FAB+): Exact mass calcd for C$_7$H$_{13}$BrNO [M + H], 206.0181. Found 206.0183.

(S)-(−)-N-α-Methylbenzyl-2-bromoacetamide (10). Following a similar protocol used for the preparation of **8**, reaction between (S)-(−)-α-methyl-benzylamine (10.64 g, 87.80 mmol) and bromoacetyl bromide (8.86 g, 43.9 mmol) gave 10.40 g (98%) of compound **11**.

(12) Weaver, W. E.; Whaley, W. M. *J. Am. Chem. Soc.* **1947**, *69*, 515−516.

Mp 108−109 °C; ^{1}H NMR (400 MHz, CDCl$_3$) δ 7.34 (5H, m, Ar—*H*), 6.73 (1H, bs, CO—N*H*), 5.10 (1H, m, NH—C*H*CH$_3$), 3.90 (1H, d, J = 14 Hz, BrCH(*H*)—CO), 3.85 (1H, d, J = 14 Hz, BrCH(*H*)—CO), 1.53 (3H, d, J = 7.0 Hz, CHC*H*$_3$); ^{13}C NMR (400 MHz, CDCl$_3$) δ 164.4, 142.3, 128.8, 127.6, 126.0, 49.6, 29.3, 21.6; FTIR (KBr) 3263 (N—H), 1648 (C=O); [α]$^{20}_D$ −26.8 (*c* 0.250, CHCl$_3$); LRMS (FAB+): Found for C$_{10}$H$_{13}$BrNO [M + H], 242.1.

Bis[(N′-tert-butylureayl)-N-ethyl-(N″-isopropylcarbamoyl-methyl)amine (H$_5$2^{iPr}). A mixture of secondary amine **7** (3.98 g, 13.2 mmol), bromide **8** (2.61 g, 14.5 mmol), and Et$_3$N (1.54 g, 15.2 mmol) in 65 mL of THF was refluxed overnight. The mixture was cooled to rt, and Et$_3$N·HBr that precipitated from the reaction mixture was removed by filtration. The pale yellow filtrate was concentrated under reduced pressure to an oil that was triturated with EtOAc to produce a white solid. The solid was isolated via filtration, washed with EtOAc, and dried under a vacuum to afford 3.96 g (75%) of H$_5$2^{iPr}. Mp 176− 178 °C; ^{1}H NMR (400 MHz, DMSO-d_6) δ 7.43 (1H, d, J = 8.2 Hz, N*H*—CH(CH$_3$)$_2$), 5.79 (2H, t, J = 5.5 Hz, N*H*—CH$_2$CH$_2$), 5.72 (2H, s, (CH$_3$)$_3$C—N*H*), 3.88 (1H, m, C*H*(CH$_3$)$_2$), 3.01 (4H, dt, J = 5.5, 6.0 Hz, NHC*H*$_2$CH$_2$), 3.00 (2H, s, C*H*$_2$—CO), 2.46 (4H, t, J = 6.0 Hz, NHCH$_2$C*H*$_2$), 1.22 (18H, s, (CH$_3$)$_3$C), 1.08 (6H, d, J = 6.6 Hz, CH-(C*H*$_3$)$_2$); ^{13}C NMR (500 MHz, CDCl$_3$) δ 170.2, 159.0, 60.7, 57.0, 50.1, 40.9, 38.4, 29.7, 22.6; FTIR (Nujol) 3404 (N—H), 3348 (N—H), 3285 (N—H), 3256 (N—H), 1673 (amide C=O), 1630 (urea C=O); HRMS (ES+): Exact mass calcd for C$_{19}$H$_{41}$N$_6$O$_3$ [M + H], 401.3240. Found 401.3230.

Bis[(N′-tert-butylureayl)-N-ethyl-(N″-cyclopentylcarbamoyl-methyl)amine (H$_5$2^{cyp}). Following a similar protocol used for the preparation of H$_5$2^{iPr}, reaction between secondary amine **7** (1.00 g, 3.31 mmol) and bromide **9** (752 mg, 3.65 mmol) gave 850 mg (60%) of H$_5$2^{cyp}. Mp 133−136 °C; ^{1}H NMR (400 MHz, DMSO-d_6) δ 7.50 (1H, d, J = 8.0 Hz, CO—N*H*—cyp), 5.76 (2H, t, J = 5.5 Hz, CO—N*H*—CH$_2$CH$_2$), 5.69 (2H, s, (CH$_3$)$_3$C—N*H*), 4.01 (1H, m, CO—NH—C*H*), 3.01 (2H, s, C*H*$_2$—CO), 3.00 (4H, dt, J = 6.0 Hz, NHC*H*$_2$CH$_2$), 2.46 (4H, t, J = 6.0 Hz, NHCH$_2$C*H*$_2$), 1.79 (2H, m, cypC*H*$_2$), 1.64 (2H, m, cypC*H*$_2$), 1.50 (2H, m, cypC*H*$_2$), 1.40 (2H, m, cypC*H*$_2$), 1.22 (18H, s, (CH$_3$)$_3$C—NH; ^{13}C NMR (500 MHz, CDCl$_3$) δ 170.8, 158.8, 60.8, 56.9, 50.8, 50.1, 38.5, 32.8, 29.7, 23.6; FTIR (Nujol) 3396 (N—H), 3335 (N—H), 3285 (N—H), 1673 (amide C=O), 1632 (urea C=O); HRMS (ES+): Exact mass calcd for C$_{21}$H$_{43}$N$_6$O$_3$ [M + H], 427.3397. Found 427.3389.

Bis[(N′-tert-butylureayl)-N-ethyl]-(N″-(S)-(−)-α-methyl-benzyl-carbamoylmethyl)amine (H$_5$2$^{S−mbz}$). A similar protocol used for the preparation of H$_5$2^{iPr} was used with the following modification: the oil obtained after concentration of the filtrate was purified by flash chromatography over silica gel, eluting with EtOAc followed by 1:19 MeOH/EtOAc. Reaction between secondary amine **7** (1.25 g, 4.15 mmol) and bromide **10** (1.63 g, 6.73 mmol) gave 1.30 g (68%) of H$_5$2$^{S−mbz}$ as a light yellow foam. ^{1}H NMR (400 MHz, DMSO-d_6) δ 8.07 (1H, d, J = 8.3 Hz, N*H*—CHCH$_3$), 7.30 (4H, m, Ar*H*), 7.21 (1H, m, Ar*H*), 5.77 (2H, t, J = 6.0 Hz, N*H*—CH$_2$CH$_2$), 5.70 (2H, s, (CH$_3$)$_3$C—N*H*), 4.94 (1H, m, NH—C*H*CH$_3$), 3.12 (1H, d, J = 16 Hz, NCH(*H*)—CO), 3.07 (1H, d, J = 16 Hz, NC*H*(H)—CO), 3.04 (4H, dt, J = 6.0, 6.0 Hz, NHC*H*$_2$CH$_2$), 2.51 (4H, t, overlapped with residual DMSO, NHCH$_2$C*H*$_2$), 1.39 (3H, d, J = 7.0 Hz, CHC*H*$_3$), 1.21 (18H, s, (CH$_3$)$_3$C); ^{13}C NMR (400 MHz, CDCl$_3$) δ 170.3, 158.6, 143.6, 128.6, 127.2, 126.2, 60.1, 56.6, 50.1, 47.6, 38.3, 29.6, 21.7; FTIR (Nujol) 3328 (N—H), 1642 (C=O); [α]$^{20}_D$ −31.6 (*c* 0.250, CHCl$_3$); HRMS (ES+): Exact mass calcd for C$_{24}$H$_{43}$N$_6$O$_3$ [M + H], 463.3397. Found 463.3395.

[(N′-tert-Butylureayl)-N-ethyl-bis(N″-isopropylcarbamoyl-methyl)-amine (H$_4$1^{iPr}). A mixture of amine **5** (4.50 g, 28.3 mmol), bromide **8** (10.69 g, 59.38 mmol), Et$_3$N (6.58 g, 65.0 mmol), and NaI (85 mg, 0.57 mmol) in 140 mL of THF was refluxed for 20 h. The dark yellow mixture, which contained Et$_3$N·HBr ppt, was brought to rt and concentrated under reduced pressure. The residue was dissolved with 140 mL

of CH_2Cl_2 and washed with H_2O (2×70 mL) and brine (1×70 mL). The organic layer was dried over Na_2SO_4, filtered, and concentrated to a yellow oil. The oil was eluted through a plug of silica gel with EtOAc followed by 1:19 MeOH/EtOAc. The white solid obtained was triturated with Et_2O, filtered, and dried under a vacuum to 5.64 g (56%). Mp 134−136 °C; ^{1}H NMR (400 MHz, DMSO-d_6) δ 7.81 (2H, d, $J =$ 8.0 Hz, NH−CH(CH_3)_2), 5.73 (1H, t, $J =$ 5.6 Hz, NH−CH_2), 5.71 (1H, s, (CH_3)_3C−NH), 3.87 (2H, m, CH(CH_3)_2), 3.07 (4H, s, CH_2−CO), 3.02 (2H, dt, $J =$ 5.9, 6.0 Hz, NHCH_2CH_2), 2.48 (2H, t, $J =$ 6.2 Hz, NHCH_2CH_2), 1.21 (9H, s, (CH_3)_3C), 1.06 (12H, d, $J =$ 6.6 Hz, CH(CH_3)_2); ^{13}C NMR (500 MHz, CDCl_3) δ 170.0, 158.2, 59.3, 57.0, 50.3, 41.2, 38.2, 29.6, 22.6; FTIR (Nujol) 3344 (N−H), 3251 (N−H), 1669 (amide C=O), 1634 (urea C=O); HRMS (FAB+): Exact mass calcd for $C_{17}H_{37}N_5O_3$ [M + H], 358.2818. Found 358.2809.

[(N'-*tert*-Butylureayl)-N-ethyl-bis(N''-cyclopentyl-carbamoyl-methyl)amine (H_4$1^{cyp}$). A similar protocol used for the preparation of H_4$1^{iPr}$ was used with the following modification: the oil obtained from the CH_2Cl_2 layer after aqueous workup was triturated with Et_2O to give the product as a white solid. Reaction between amine **5** (2.62 g, 16.5 mmol) and bromide **9** (7.14 g, 34.6 mmol) afforded 5.37 g (80%) of H_4$1^{cyp}$. Mp 115−117 °C; ^{1}H NMR (400 MHz, DMSO-d_6) δ 7.89 (2H, d, $J =$ 7.6 Hz, CO−NH−cyp), 5.71 (1H, t, $J =$ 5.6 Hz, CO−NH−CH_2CH_2), 5.68 (1H, s, (CH_3)_3C−NH), 4.01 (2H, m, CO−NH−CH), 3.09 (4H, s, CH_2−CO), 3.00 (2H, dt, $J =$ 5.9, 6.1 Hz, NHCH_2CH_2), 2.49 (2H, t, $J =$ 6.4 Hz, NHCH_2CH_2), 1.78 (4H, m, cypCH_2), 1.64 (4H, m, cypCH_2), 1.49 (4H, m, cypCH_2), 1.40 (4H, m, cypCH_2), 1.21 (9H, s, (CH_3)_3C−NH); ^{13}C NMR (500 MHz, CDCl_3) δ 170.5, 158.3, 59.3, 56.9, 51.0, 50.2, 38.2, 30.0, 23.7; FTIR (Nujol) 3340 (N−H), 3278 (N−H), 1671, 1657, 1621; HRMS (ES+): Exact mass calcd for $C_{21}H_{40}N_5O_3$ [M + H], 410.3131. Found 410.3120.

[(N'-*tert*-Butylureayl)-N-ethyl]-bis(N''-(S)-(−)-α-methyl-benzyl-carbamoylmethyl)amine (H_4$1^{S-mbz}$). A similar protocol used for the preparation of H_4$1^{iPr}$ was used with the following modification: the oil obtained after extraction and drying of the CH_2Cl_2 was purified by flash chromatography over silica gel, eluting with 1:1 acetone/hexanes. Reaction between amine **5** (0.79 g, 5.0 mmol) and bromide **10** (2.52 g, 10.4 mmol) gave 1.43 g (60%) of H_4$1^{S-mbz}$ as a white foam. ^{1}H NMR (400 MHz, DMSO-d_6) δ 8.46 (2H, d, $J =$ 8.2 Hz, NH−CHCH_3), 7.33−7.26 (8H, m, ArH), 7.23−7.19 (2H, m, ArH), 5.76 (1H, t, $J =$ 5.5 Hz, NH−CH_2CH_2), 5.71 (1H, s, (CH_3)_3C−NH), 4.96 (2H, m, NH−CHCH_3), 3.22 (2H, d, $J =$ 16 Hz, NCH(H)−CO), 3.18 (2H, d, $J =$ 16 Hz, NCH(H)−CO), 3.07 (2H, dt, $J =$ 6.1, 6.1 Hz, NHCH_2CH_2), 2.53 (2H, t, $J =$ 6.1 Hz, NHCH_2CH_2), 1.37 (6H, d, $J =$ 7.0 Hz, CHCH_3), 1.21 (9H, s, (CH_3)_3C); ^{13}C NMR (500 MHz, CDCl_3) δ 170.0, 158.0, 143.4, 128.6, 127.3, 126.1, 59.1, 56.8, 50.3, 48.5, 37.9, 29.5, 21.8; FTIR (Nujol) 3284 (N−H), 1645 (C=O); [α]$^{20}_D$ −40.8 (c 0.250, CHCl_3); HRMS (ES+): Exact mass calcd for $C_{27}H_{40}N_5O_3$ [M + H], 482.3131. Found 482.3132.

Potassium {Bis[(N'-*tert*-butylureayl)-N-ethyl-(N''-isopropylcarba-moylmethyl)-aminato-cobaltate(II)} K[Co^{II}H_2$2^{iPr}$]. A solution of the ligand H_5$2^{iPr}$ (150 mg, 0.374 mmol) dissolved in 6 mL of anhydrous DMA was treated with solid KH (45 mg, 1.1 mmol). The mixture was stirred until gas evolution ceased. Co(OAc)_2 (66 mg, 0.37 mmol) was added to the pale yellow solution, and stirring was continued for 30 min. The blue mixture was filtered to remove KOAc (74 mg, 100%), which was washed with DMA. Vapor diffusion of Et_2O into the filtrate produced aqua blue crystals, which were filtered, washed with Et_2O, and dried under a vacuum to 173 mg (79%). Anal. Calcd (found) for K[Co^{II}H_2$2^{iPr}$]·DMA, $C_{23}H_{46}CoKN_7O_4$: C, 47.41 (47.29); H, 7.96 (8.14); N, 16.83 (17.14); FTIR (Nujol, cm^{-1}) ν(NH) 3400, ν(CO) 1658, 1610, 1588, 1572; λ_{max} (DMA, nm (ϵ, M^{-1} cm^{-1})) 388 (34), 594 (160), 614 (sh); X-band EPR (DMA, 4 K) $g =$ 4.0, 2.0.

Potassium {bis[(N'-*tert*-butylureayl)-N-ethyl-(N''-isopropylcarba-moylmethyl)-aminato-cobaltate(II)} K[Co^{II}H_2$1^{iPr}$] was prepared following the procedure outlined for K[Co^{II}H_2$2^{iPr}$] using H_4$1^{iPr}$ (200 mg, 0.559 mmol), 8 mL of anhydrous DMA, KH (67 mg, 1.7 mmol), and

Co(OAc)_2 (99 mg, 0.56 mmol). After the reaction was completed, 109 mg (99%) of KOAc were removed via filtration. Vapor diffusion of Et_2O into the filtrate produced aqua blue crystals, which were filtered, washed with Et_2O, and dried under a vacuum to 244 mg (81%). Anal. Calcd (found) for K[Co^{II}H1^{iPr}]·DMA, $C_{21}H_{41}CoKN_6O_4$: C, 46.74 (46.35); H, 7.66 (7.83); N, 15.57 (15.51); FTIR (Nujol, cm^{-1}) ν(NH) 3425, ν(CO) 1645, 1609, 1578, 1566; λ_{max} (DMA, nm (ϵ, M^{-1} cm^{-1})) 385 (23), 588 (180), 608 (160); X-band EPR (DMA, 4 K) $g =$ 4.0, 2.0.

Potassium {bis[(N-isopropylcarbamoylmethyl)aminato]cobaltate-(II)} K[Co^{II}0^{iPr}] was prepared following the procedure outlined for K[Co^{II}H_2$2^{iPr}$] using H_3$0^{iPr}$ (201.6 mg, 0.641 mmol), 10 mL of anhydrous DMA, KH (78.2 mg, 1.95 mmol), and Co(OAc)_2 (116 mg, 0.655 mmol). KOAc (123 mg, 97%) was removed via filtration, and vapor diffusion of Et_2O into the filtrate produced 298 mg (94%) of the product as blue crystals. Anal. Calcd (found) for K[Co^{II}H1^{iPr}]·DMA, $C_{19}H_{36}$CoKN_5O_4: C, 45.96 (46.23); H, 7.31 (7.39); N, 14.10 (14.02); FTIR (Nujol, cm^{-1}) 1647, 1578, 1266, 1155; λ_{max} (DMA, nm (ϵ, M^{-1} cm^{-1})) 401 (17), 583 (160), 606 (150); X-band EPR (DMA, 4 K) $g =$ 4.0, 2.0.

Potassium {bis[(N'-*tert*-butylureayl)-N-ethyl-(N''-isopropylcarba-moylmethyl)-aminato(hydroxo)cobaltate(III)} K[Co^{III}H_2$2^{iPr}$(OH)]. Method A: K[CoH_2$2^{iPr}$] (50 mg, 0.10 mmol) dissolved in 2.0 mL of DMA was treated with 1.2 mL of O_2 (0.051 mmol at $T =$ 295 K and $P =$ 0.982 atm). After 1 h of stirring the volume was reduced by half under reduced pressure and treated with enough diethyl ether to precipitate the product, as a red solid (47 mg, 94%). Method B: A solution of the ligand H_5$2^{iPr}$ (100 mg, 0.250 mmol) dissolved in 4 mL anhydrous DMA was treated with solid KH (30 mg, 0.75 mmol). The mixture was stirred until gas evolution ceased. Co(OAc)_2 (44 mg, 0.25 mmol) was added to the pale yellow solution, and stirring was continued for 30 min. The aqua blue mixture was treated with dry O_2 (0.55 equiv, 3.3 mL, 0.14 mmol), and the resulting dark red mixture stirred for 1 h. The mixture was placed under a vacuum for a few minutes to remove unreacted O_2. KOAc was then removed by filtration, and the filtrate was concentrated in vacuo. Treatment of the residue with Et_2O produced a dark red solid that was filtered, washed with Et_2O, and dried under a vacuum to 120 mg (94%). Anal. Calcd (found) for K[Co^{III}H_2$2^{iPr}$(OH)], $C_{19}H_{38}CoKN_6O_4$: C, 44.52 (44.83); H, 7.47 (7.66); N, 16.40 (16.72); FTIR (Nujol, cm^{-1}) ν(^{16}OH/^{18}OH) 3662/3651, ν(NH) 3300, 3190, ν(CO) 1588; λ_{max} (DMF, nm (ϵ, M^{-1} cm^{-1})) 295 (4700), 394 (sh), 475 (1400), 794 (160).

Potassium {tris[(N'-*tert*-butylureayl)-N-ethyl]aminato(hydroxo)-cobaltate(III)} K[Co^{III}H_2 buea(OH)]. A solution of H_6buea (105.0 mg, 0.237 mmol) in 5 mL of anhydrous DMA was treated with solid KH (29.3 mg, 0.730 mmol) under an Ar atmosphere. The mixture was stirred until gas evolution was completed. Co(OAc)_2 (42.6 mg, 0.241 mmol) was added to the pale yellow solution, and stirring was continued for 30 min. The mixture was filtered to remove KOAc (43.0 mg, 92%), the dark blue filtrate was treated with dry dioxygen (3.3 mL, 0.13 mmol, $T =$ 293.7 K, $P =$ 0.98 atm), and the resulting red solution was stirred for 1 h. The solution was filtered, and a red solid was obtained after vapor diffusion of Et_2O into the filtrate. The solid was washed with Et_2O and dried under a vacuum to afford the product in 78% yield (103 mg). The spectroscopic properties of the complex [Co^{III}H_3-buea(OH)]$^-$ matched those previously described for the complex prepared from water.[5a,d]

K[Co^{III}H_2$2^{iPr}$(^{18}OH)] from ^{18}O_2. A solution of the ligand H_5$2^{iPr}$ (100 mg, 0.250 mmol) dissolved in 4 mL of anhydrous DMA was treated with solid KH (30 mg, 0.75 mmol). The mixture was stirred until gas evolution ceased. Co(OAc)_2 (44 mg, 0.25 mmol) was added to the pale yellow solution, and stirring was continued for 30 min. The aqua blue mixture was treated with ^{18}O_2 (3.4 mL, 0.14 mmol at $T =$ 293.5 K, $P =$ 0.99 atm), and the resulting mixture stirred for 1 h. The mixture was placed under a vacuum for a few minutes to remove any unreacted ^{18}O_2. KOAc was then removed by filtration, and the filtrate was concentrated in vacuo. Treatment of the residue with Et_2O produced a dark

Table 1. Crystallographic Data for K[Co^{II}H$_2$**0**^{iPr}]·DMA, K[Co^{II}H**1**^{iPr}]·0.5DMA·0.25Et$_2$O·0.25H$_2$O, and K[Co^{II}H$_2$**2**^{iPr}]·Et$_2$O

salt	K[Co^{II}H$_2$**0**^{iPr}]·DMA	K[Co^{II}H**1**^{iPr}]·0.5DMA·0.25Et$_2$O·0.25H$_2$O	K[Co^{II}H$_2$**2**^{iPr}]·Et$_2$O
molecular formula	C$_{19}$H$_{36}$CoKN$_5$O$_4$	C$_{20}$H$_{39.5}$CoKN$_{5.5}$O$_4$	C$_{23}$H$_{47}$CoKN$_6$O$_4$
fw	496.56	519.10	569.70
T (K)	100(2)	100(2)	100(2)
space group	$P1$	$P\bar{1}$	$Pna2_1$
a (Å)	12.768(4)	10.918(2)	21.116(4)
b (Å)	14.914(5)	16.900(4)	10.467(2)
c (Å)	15.3777(4)	29.431(6)	26.338(5)
α (deg)	115.77(8)	88.622(6)	90
β (deg)	102.215(8)	83.727(5)	90
γ (deg)	101.032(8)	86.822(6)	90
Z	4 ($Z' = 2$)	8 ($Z' = 4$)	8 ($Z' = 2$)
V (Å^3)	2434(1)	5389(2)	5821.3(19)
δ_{calcd} (Mg/m^3)	1.352	1.280	1.300
R^a	0.0357	0.0900	0.0602
R_w ^{b}	0.0986	0.2661	0.1530
GOF^c	1.003	1.001	1.012

^{a} $R = [\sum|\Delta F|/\sum|F_o|]$. ^{b} $R_w = \{\sum[\omega(F_o^2 - F_c^2)^2]/\sum[\omega(F_o^2)^2]\}^{1/2}$. ^{c} Goodness of fit on F^2.

red solid that was filtered, washed with Et$_2$O, and dried under a vacuum to 103 mg (82%). FTIR (Nujol, cm^{-1}) ν(^{18}OH) 3651.

[Bu$_4$N][Co^{III}H$_3$buea(^{18}OH)] from ^{18}O$_2$. A solution of [Bu$_4$N][Co^{II}H$_3$-buea] (50 mg, 0.074 mmol) in 10 mL of CH$_3$CN was treated with ^{18}O$_2$ (1.3 mL, 0.037 mmol at T = 295.5 K, P = 0.98 atm), and the resulting mixture stirred for 1 h. The mixture was placed under a vacuum, the volume was reduced to ~3 mL, and diethyl ether was added until a dark red precipitate appeared. The solid was separated via filtration, washed with diethyl ether, and dried (46 mg, 90%).

Tetraethylammonium {Tris[(*N′-tert*-butylureayl)-*N*-ethyl]aminato-(cyano)cobaltate(II)} [Et$_4$N]$_2$[Co^{II}H$_2$0**^{iPr}(CN)].** A solution of K[Co^{II}**0**]·DMA (51 mg, 0.103 mmol) in 3 mL of DMA was treated with Et$_4$NCN (18.9 mg, 1.114 mmol) under an argon atmosphere. The blue solution immediately turned violet and was stirred for 1 h. The solution was filtered, and vapor diffusion of Et$_2$O into the filtrate produced a mixture of violet crystals and a violet amorphous solid. A crystal was chosen and analyzed by X-ray diffraction. Repeated attempts to obtain a satisfactory element analysis were unsuccessful. FTIR (Nujol, cm^{-1}) 2089, 1553, 1250, 1131, 1005; λ_{max} (DMA) 541 nm; X-band EPR (DMA, 77 K) g = 4.0

Physical Methods. NMR spectra were recorded on Bruker Avance 400 and 500 MHz spectrometers equipped with Silicon Graphics workstations. Mass spectra were obtained on either a VG ZAB high-resolution double-focusing instrument or a VG Autospec-Q tandem hybrid of EBEqQ configuration. Electronic spectra were recorded with a Cary 50 spectrophotometer using a 1.00 mm quartz cuvette. FTIR spectra were collected on a Mattson Genesis series FTIR instrument with values reported in wavenumbers. Perpendicular-mode X-band EPR spectra were collected using a Bruker EMX spectrometer equipped with an ER041XG microwave bridge. Spectra for EPR samples were collected using the following spectrometer settings: attenuation = 25 dB, microwave power = 0.638 mW, frequency = 9.47 GHz, sweep width = 5000 G, modulation amplitude = 10.02 G, gain = 1.00 × 10^3, conversion time = 81.920 ms, time constant = 655.36 ms, and resolution = 1024 points. Low-temperature (4 K) spectra were obtained using an Oxford Instrument liquid He quartz cryostat. Cyclic voltammetric experiments were conducted using a BAS CV 50W (Bioanalytical Systems Inc., West Lafayette, IN) voltammetric analyzer following methods previously described.[11d] A 1.0 mm glassy carbon electrode was used as the working electrode to measure the cyclic voltammograms (CV) at scan velocities between 0.1 and 1.0 V·s^{-1}. A ferrocinium/ferrocene couple ([Cp$_2$Fe]$^{+/0}$) was used to monitor the reference electrode (Ag$^+$/Ag) and was observed at $E_{1/2}$ = 0.050 V with ΔE_p = 0.10 V and i_{pa}·i_{pc}^{-1} = 0.85 at an ν = 0.1 V·s^{-1} in DMF under ambient temperature.

Crystallography. General Methods. Intensity data for the compounds were collected using a Bruker APEX CCD area detector[13] mounted on a Bruker D8 goniometer using graphite-monochromated Mo Kα radiation (λ = 0.710 73 Å). The data were collected at 100(2) K. For each structure, intensity data were measured as a series of ω oscillation frames: for K[CoH_2**2**^{iPr}]·C$_4$H$_{10}$O data were collected at 0.3° for 15 s/frame; for K[Co^{II}H**1**^{iPr}]·(C$_4$H$_{10}$O)$_{0.25}$·(C$_4$H$_9$NO)$_{0.50}$·(H$_2$O)$_{0.25}$ and [Et$_4$N]$_2$[Co^{II}**0**(CN)] data were collected for 60 s/frame; and for K[Co^{II}**0**]·DMA data were obtained for 5 s/frame. The structures were solved by direct methods and refined by full-matrix least-squares methods on F^2.[14] Hydrogen atom positions were initially determined by geometry and refined by a riding model. Non-hydrogen atoms were refined with anisotropic displacement parameters. Hydrogen atom displacement parameters were set to 1.2 (1.5 for methyl groups) times the displacement parameters of the bonded atoms. The displacement ellipsoids are drawn at the 50% probability level. The data were corrected for absorption by the semiempirical method.[15] Space groups were determined by statistical methods and verified by subsequent refinement. Partial crystallographic data are presented in Table 1. Full refinement parameters can be found in the CIFs that are included in the Supporting Information.

K[CoH_2**2**^{iPr}]·C$_4$H$_{10}$O crystallized in the orthorhombic space group $Pna2_1$ with cell parameters determined from a nonlinear least-squares fit of 9757 peaks in the range 2.30° < θ < 26.00°. A total of 48 815 data were measured in the range 1.93° < θ < 26.00°. Minimum and maximum transmission factors of 0.8368 and 0.8867 were used in the adsorption correction. This structure contains two formula units per asymmetric unit. The solvent molecules were significantly disordered and modeled using the Squeeze program.[16] The Flack parameter indicated that the sample suffered from some inversion twinning. A total of 542 parameters were refined against one space group restraint and 11 400 data to give wR(F^2) = 0.1530 and S = 1.012 for weights of w = 1/[σ^2(F^2) + (0.1160P)^2], where P = [F_o^2 + 2F_c^2]/3. The final R(F) was 0.0602 for the 9926 observed, [$F > 4\sigma(F)$], data. The largest shift/s.u. was 0.001 in the final refinement cycle. The final difference map had maxima and minima of 1.908 and −0.478 e/Å^3, respectively. The absolute structure was determined by refinement of the Flack

(13) (a) Data Collection: *SMART Software Reference Manual*; Bruker-AXS: Madison, WI, 1994. (b) Data Reduction: *SAINT Software Reference Manual*; Bruker-AXS: Madison, WI, 1995.
(14) (a) Sheldrick, G. M. *SHELXTL Version 5 Reference Manual*; Bruker-AXS: Madison, WI, 1994. (b) *International Tables for Crystallography*; Kluwer Academic Publishers: Norwell, MA, 1995; Vol. C.
(15) Sheldrick, G. M. *SADABS: Program for Empirical Absorption Correction of Area Detector Data*; University of Göttingen: Germany, 2000.
(16) van der Sluis, P.; Spek, A. L. *Acta Crystallogr.*, *Sect. A* **1990**, *46*, 194−201.

parameter.[17] The polar axis restraints were taken from Flack and Schwarzenbach.[18]

K[CoII**1**iPr]·(C$_4$H$_{10}$O)$_{0.25}$·(C$_4$H$_9$NO)$_{0.50}$·(H$_2$O)$_{0.25}$ crystallized in the triclinic space group $P\bar{1}$, with cell parameters determined from a nonlinear least-squares fit of 3874 peaks in the range 2.18° < θ < 26.00°. The first 50 frames were repeated at the end of data collection and yielded a total of 136 peaks showing a variation of −0.04% during the data collection. A total of 33 998 data were measured in the range 1.86° < θ < 26.00°. Minimum and maximum transmission factors of 0.7339 and 0.9446 were used in the adsorption correction. A total of 1338 parameters were refined against 659 restraints and 20 403 data to give wR(F^2) = 0.2661 and S = 1.001 for weights of $w = 1/[\sigma^2(F^2) + (0.1400P)^2]$, where $P = [F_o^2 + 2F_c^2]/3$. The final R(F) was 0.0900 for the 10 378 observed, [$F > 4\sigma(F)$], data. The largest shift/s.u. was 0.010 in the final refinement cycle. The final difference map had maxima and minima of 1.246 and −0.731 e/Å^3, respectively. There were four cations and anions, two sites of DMA solvent, two sites of diethyl ether (both near crystallographic centers of symmetry), and one water molecule per asymmetric unit. Three of the anions contained regions of disorder and were modeled in two orientations. The occupancies for O(1A), N(3A), C(9A)−C(12A) refined to 0.613(15) and 0.387(15). The occupancies for C(15B)−C(17B) refined to 0.607(19) and 0.393(19). The occupancies for C(15D)−C(17D) refined to 0.519-(8) and 0.481(8). The DMA molecule, E, was disordered and modeled in two orientations with occupancies of 0.590(12) and 0.410(12). Restraints on the positional and displacement parameters of the disordered atoms were required.
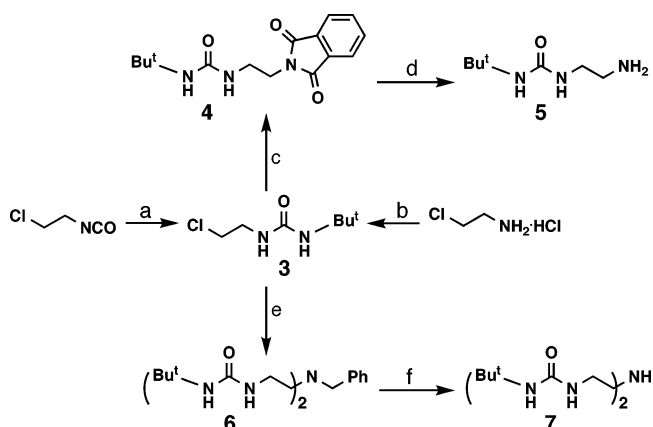
K[CoII**0**]·DMA crystallized in the triclinic space group $P1$, with cell parameters determined from nonlinear least-squares fits to 6234 peaks in the range 2.34° < θ < 26.00°. A total of 21 098 data were collected in the range 2.34° < θ < 26.00°. Minimum and maximum transmission factors of 0.690 and 0.855 were used in the adsorption correction. There were two formula units per asymmetric unit of the cell. Both solvent molecules were disordered and were modeled in two orientations. The occupancies of the solvent molecules refined to S: 0.656(3) and 0.344-(3); T: 0.852(3) and 0.148(3) for the unprimed and primed atoms. Restraints on the positional and displacement parameters of the solvent atoms were required. A total of 639 parameters were refined against 432 restraints and 4533 data to give wR(F^2) = 0.0986 and S = 1.003 for weights of $w = 1/\sigma^2(F^2) + (0.0600P)^2 + 1.6600P$, where $P = [F_o^2 + 2F_c^2]/3$. The final R(F) was 0.0357 for the 8553 observed, [$F > 4\sigma(F)$], data. The largest shift/s.u. was 0.014 in the final refinement cycle. The final difference map had maxima and minima of 0.987 and −0.782 e/A^3.

[Et$_4$N]$_2$[CoII**0**(CN)] crystallized in the triclinic space group $P2_1/n$ with cell parameters determined from nonlinear least-squares fit of 4395 peaks in the range 2.27° < θ < 26.00°. A total of 17 218 data were measured in the range 2.05° < θ < 23.26°. Minimum and maximum transmission factors of 0.836 and 0.986 were used in the adsorption correction. The intensity date were truncated at 0.9 Å resolution because data in the high resolution shells had R(int) > 0.25. The solvent was badly disordered. The best model for the solvent was determined using the Squeeze program.[16] A total of 388 parameters were refined against 5756 data to give wR(F^2) = 0.2064 and S = 1.075 for weights of $w = 1/\sigma^2(F^2) + (0.0940P)^2 + 13.0000P$, where $P = [F_o^2 + 2F_c^2]/3$. The final R(F) was 0.0783 for the 4301 observed, [$F > 4\sigma(F)$], data. The largest shift/s.u. was 0.000 in the final refinement cycle. The final difference map had maxima and minima of 1.054 and −0.763 e/A^3.

Results and Discussion

Design Considerations and Ligand Syntheses. Exploring the regulatory effects of H-bonds on metal ion reactivity neces-

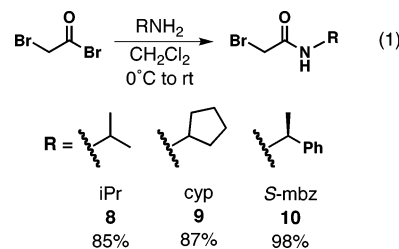(17) Flack, H. D. *Acta Crystallogr., Sect A* **1983**, *39*, 876−881.
(18) Flack, H. D.; Schwarzenbach, D. *Acta Crystallogr., Sect. A* **1988**, *44*, 499−506.

Scheme 1 ^{a}

^{a} Conditions: (a) Bu^{t}NH$_2$, Et$_2$O, 0 °C to rt, 86%; (b) Bu^{t}NCO, NaHCO$_3$, THF, 81%; (c) potassium phthalimide, DMF, 120 °C, 73%; (d) H$_2$NNH$_2$·H$_2$O, EtOH, Δ, >98%; (e) BnNH$_2$, Et$_3$N, NaI, THF, Δ, 77%; (f) cyclohexene, 10% Pd/C, MeOH, Δ, 86%.

sitates having metal complexes with similar primary coordination spheres but variable H-bond arrangements in their secondary coordination environments. Such metal complexes can be generated from an appropriate series of ligands whose design takes into account both coordination spheres. The modular nature of the syntheses of tripodal compounds provides the opportunity to make changes in ligand structures via manipulation of the functional groups within each arm of the tripod.[19]

We previously have shown that the urea-based tripodal ligand [H$_3$buea]$^{3-}$ provides a network of three H-bond donors around a metal ion,[5] while carboxamide-based ligands such as [**0**^{R}]$^{3-}$ provide none.[11] The intermediate members of the series with 0−3 H-bond donors and highly anionic primary coordination environments can be obtained by preparing hybrids of these parent ligands (Figure 1). Besides varying the H-bond network around a metal ion, these hybrids can also be used to influence the overall cavity architecture through the choice of the R groups attached to the carboxamide arms.

To synthesize the hybrid ligands we adopted a convergent synthetic strategy by which the urea "arms" would be installed on the amine nitrogen atom that would ultimately become the apical nitrogen donor of the tripodal ligand. Ligands containing two urea arms, thus two H-bond donors, would come from alkyating the secondary amine **7** (Scheme 1) with an *N*-alkylbromoacetamide (eq 1). The primary amine **5** could be

alkylated in a similar fashion with 2 equiv of an *N*-alkylbromo-acetamide to give the tripodal ligands with a single H-bond donating ureayl arm. Both of these amines would be derived

(19) Bellemin-Laponnaz, S.; Gade, L. H. *Angew. Chem., Int. Ed.* **2002**, *41*, 3473−3475.

from the common intermediate 1-*tert*-butyl-3-(2-chloroethyl)-urea (**3**).
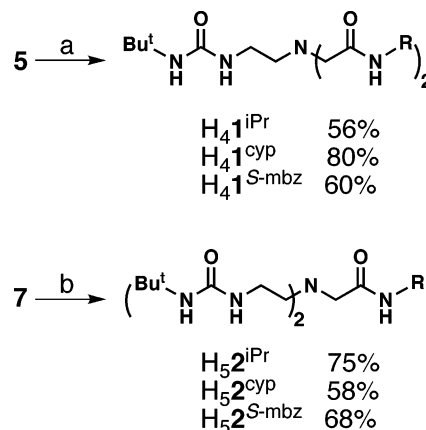
Acylation of the commercially available starting compound 2-chloroethylamine hydrochloride with *tert*-butyl isocyanate afforded **3** in 81% yield following recrystallization from Et₂O (Scheme 1). Alternatively, **3** was prepared from 2-chloroethyl isocyanate and *tert*-butylamine in 86% yield. This compound (2 equiv) was used to alkylate benzylamine, producing the *N*-benzyl tertiary amine **6** in 77% yield. Our initial attempts to debenzylate by catalytic transfer hydrogenolysis using ammonium formate[20] resulted in clean and efficient cleavage of the benzyl group as indicated by TLC and ^{1}H NMR spectroscopy. However, the similar solubility properties of the product **7** and ammonium formate made purification difficult and usually incomplete. By replacing ammonium formate with cyclo-hexene[21] as the hydrogen atom source, debenzylation was accomplished with pure product obtained in 86% yield.

Preparation of the primary amine **5** needed for ligands containing only one H-bond donor made use of the Gabriel amine synthesis.[22] Chloroethylurea **3** was converted to the phthalimidourea **4** using potassium phthalimide in DMF. The product was obtained in 73% yield following recrystallization of the crude product from acetone–hexane. Hydrazinolysis of **4** under standard conditions with hydrazine monohydrate in refluxing EtOH provided the desired primary amine **5** in greater than 98% yield.[23] Amine **5** was isolated as a hygroscopic white solid that turns to a pale yellow oil upon standing under ambient conditions.

The amide arms of the unsymmetrical ligands are derived from *N*-alkylbromoacetamide derivatives **8**–**11**.[24] We prepared three compounds in high yields from bromoacetyl bromide and 2 equiv of a primary amine in CH₂Cl₂: isopropyl (85%), cyclo-pentyl (87%), and (*S*)-α-methylbenzyl (98%) (eq 1). The choice of these R groups was based on their use in the previously prepared symmetrical carboxamide-based compound, H₃**0**[R].[11]

Amine **6** was used for the preparation of compounds with a single H-bond donor. Alkylating this amine with 2 equiv of *N*-alkylbromoacetamides **8**–**11** produced compounds H₄**1**[R] (Scheme 2). These reactions were done in THF with Et₃N as base and employed the use of catalytic amounts of NaI. Compounds H₄**1**[R] were prepared in yields ranging from 56 to 80%. Similarly, ligands with two H-bond donors were prepared by reacting amine **7** with *N*-alkylbromoacetamides **8**–**11** (Scheme 2). These reactions were carried out in the presence of Et₃N in refluxing THF. Yields for these reactions, which resulted in H₅**2**[R] containing one carboxamide and two urea groups, ranged from 58 to 75%.

Preparation and Molecular Structures of [Co^II H₂2^*i*Pr]⁻, [Co^II H1^*i*Pr]⁻, and [Co^II 0^*i*Pr]⁻. This series of Co(II) complexes was made to examine how the ligand influences the chemistry of metal ions. Ligands [H₂**2**[iPr]]³⁻, [H**1**[iPr]]³⁻, and [**0**[iPr]]³⁻ were targeted because we showed previously that tri(carboxamide) tripods with appended isopropyl groups provided suitable cavities for exogenous ligand binding.[11b,c,25] The complexes were prepared by deprotonating H₅**2**[iPr], H₄**1**[iPr], and H₃**0**[iPr] with 3 equiv

(20) Adger, B. M.; O'Farrell, C.; Lewis, N. J.; Mitchell, M. B. *Synthesis* 53–55.
(21) Overman, L. E.; Mendelson, L. T.; Jacobsen, E. J. *J. Am. Chem. Soc.* **1983**, *105*, 6629–6637.
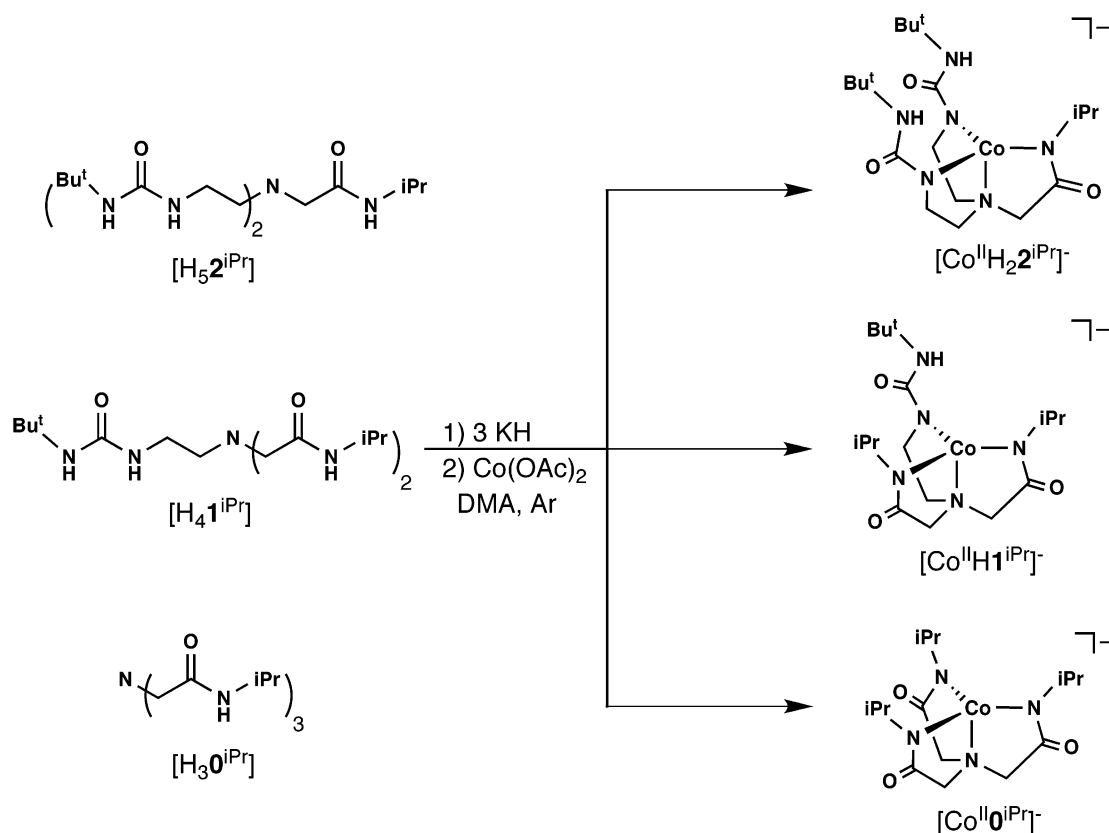(22) Gabriel, S. *Ber. Dtsch. Chem. Ges.* **1887**, *20*, 2224–2236.
(23) Ing, H. R.; Manske, R. H. F. *J. Chem. Soc.* **1926**, 2348–2351.
(24) Weaver, W. E.; Whaley, W. M. *J. Am. Chem. Soc.* **1947**, *69*, 515–516.

Scheme 2 [a]

H₄**1**[iPr]	56%
H₄**1**[cyp]	80%
H₄**1**[S-mbz]	60%

H₅**2**[iPr]	75%
H₅**2**[cyp]	58%
H₅**2**[S-mbz]	68%

[a] Conditions: (a) **8**–**10**, Et₃N, THF, NaI (cat.), Δ; (b) **8**–**10**, Et₃N, THF, Δ.

(equiv) of KH under an argon atmosphere to produce the ligands [H₂**2**[iPr]]³⁻, [H**1**[iPr]]³⁻, and [**0**[iPr]]³⁻ (Scheme 3). The addition of solid Co(OAc)₂ produced a blue solution and a white precipitate (KOAc, 2 equiv). The potassium salts of [Co^II H₂**2**[iPr]]⁻, [Co^II H**1**[iPr]]⁻, and [Co^II **0**[iPr]]⁻ were isolated in greater than 75% yield after recrystallization from DMA (or DMF)-diethyl ether and were stable for weeks when stored in a dry, anaerobic environment.

Single-crystal X-ray diffraction investigations on K[Co^II H₂**2**[iPr]], K[Co^II H**1**[iPr]], and K[Co^II **0**[iPr]]⁻ confirm that the cobalt(II) centers have similar primary coordination spheres. Table 2 summarizes selected distances and angles for each structure, and Figure 2 shows the thermal ellipsoid diagrams for [Co^II H₂**2**[iPr]]⁻, [Co^II H**1**[iPr]]⁻, and [Co^II **0**[iPr]]⁻. Single crystals of [Co^II H₂**2**[iPr]]⁻ and [Co^II **0**[iPr]]⁻ contained two crystallographically independent, but chemically equivalent, anions in the asymmetric unit; [Co^II H**1**]⁻ had four independent anions, of which three contained regions of disorder. Selected metrical data for each complex are presented in Table 2 as average values.

Examination of the molecular structures reveals that each complex is four-coordinate with a trigonal monopyramidal (TMP) geometry. The trigonal planes of the complexes are defined by the deprotonated urea/amide nitrogen atoms, with the amino nitrogen atom N1 as the apical donor, which is positioned nearly perpendicular to the trigonal plane. The three Co(II) complexes have similar metrical parameters; for instance, the average Co1–N1 distance for [Co^II **0**[iPr]]⁻ is 2.059(2) Å, while [Co^II H**1**[iPr]]⁻ and [Co^II H₂**2**[iPr]]⁻ have values of 2.070(7) Å and 2.073(4) Å, respectively. In [Co^II H₂**2**[iPr]]⁻ and [Co^II H**1**[iPr]]⁻ the Co–N_urea and Co–N_amidate bond distances are statistically equivalent, with average distances of 1.945(3) Å and 1.948(7) Å, respectively. The Co–N_amidate bond lengths in [Co^II **0**[iPr]]⁻ are slightly longer, with an average bond distance of 1.967(2) Å. This value is nearly the same as the 1.972(2) Å bond lengths observed previously in [Co^II **0**[But]]⁻.[11d]

The X-ray structural results demonstrate that the tripodal ligands in complexes [Co^II H₂**2**[iPr]]⁻, [Co^II H**1**[iPr]]⁻, and [Co^II **0**[iPr]]⁻ bind in similar ways, which is further illustrated by the structural overlays shown in Figure 3. The depictions include only the metal-binding sites of the three complexes and confirms that the primary coordination spheres around the Co(II) centers are nearly identical. The similarities in structure are indicated by a root-mean square value of 0.07 Å.

Scheme 3

Table 2. Selected Bond Distances and Angles for [Co^{II}H$_2$**2**^{iPr}]$^-$, [Co^{II}H**1**^{iPr}]$^-$, and [Co^{II}**0**^{iPr}]$^-$ [a]

distances (Å) or angles (deg)	[Co^{II}H$_2$**2**^{iPr}]$^-$	[Co^{II}H**1**^{iPr}]$^-$	[Co^{II}**0**^{iPr}]$^-$
Co1−N1	2.073(4)	2.070(7)	2.059(2)
Co1−N2	1.945(3)	1.944(6)	1.972(2)
Co1−N3	1.946(3)	1.956(8)	1.962(2)
Co1−N4	1.944(4)	1.944(6)	1.968(2)
N1−Co1−N2	87.1(1)	87.0(3)	84.91(7)
N1−Co1−N3	85.9(1)	84.6(3)	85.16(7)
N1−Co1−N4	85.9(1)	85.9(3)	84.75(7)
N2−Co1−N3	118.9(2)	116.6(5)	119.20(7)
N2−Co1−N4	125.2(1)	121.1(3)	120.57(7)
N3−Co1−N4	114.6(1)	120.9(5)	117.93(7)

[a] There are two independent anions in the asymmetric units for [Co^{II}H$_2$**2**^{iPr}]$^-$, [Co^{II}**0**^{iPr}]$^-$ and four for [Co^{II}H**1**^{iPr}]$^-$. Metrical parameters are reported as averages.

The molecular structures also reveal that the complexes have different secondary coordination spheres. In [Co^{II}H$_2$**2**^{iPr}]$^-$ and [Co^{II}H**1**^{iPr}]$^-$ the appended urea and isopropyl amidate groups form the desired hybrid cavities, encompassing the vacant axial coordination sites. In both complexes, the urea N−H vectors are positioned within the cavity, proximal to the Co(II) centers. For [Co^{II}H$_2$**2**^{iPr}]$^-$, two H-bond donors exist within the secondary coordination sphere, whereas [Co^{II}H**1**^{iPr}]$^-$ has only one. Note also that the appended isopropyl groups of the amide function-alities adopt conformations in which the methyl substituents surround the metal centers and thus serve as scaffolds for the cavity. Moreover, the methine hydrogen atoms face outward from the cavity toward the carboxamide carbonyl groups. This arrangement of the isopropyl groups is also observed in [Co^{II}**0**^{iPr}]$^-$ and creates a cavity without H-bond donors. This orientation of groups is found in other complexes of [**0**^{iPr}]$^{3-}$

and occurs to minimize the steric interactions between the isopropyl and carbonyl groups of each amide moiety.[11b,c]

Spectroscopic Properties of [Co^{II}H$_2$2**^{iPr}]$^-$, [Co^{II}H**1**^{iPr}]$^-$, and [Co^{II}**0**^{iPr}]$^-$.** The electronic absorbance spectra for the three complexes measured in DMA are shown in Figure 4A. The spectra are characterized by three general bands at λ_{max} ~390, 590, and 610 nm with extinction coefficients of less than 200 M^{-1} cm^{-1}. Each spectrum also contains a broad shoulder at $\lambda_{max} \cong 700$ nm. These spectral properties agree with those reported previously for Co(II) complexes with TMP geometry,[11d] suggesting that the cavities remain unoccupied in solution. The electron paramagnetic resonance (EPR) spectra of [Co^{II}H$_2$**2**^{iPr}]$^-$, [Co^{II}H**1**^{iPr}]$^-$, and [Co^{II}**0**^{iPr}]$^-$ also resemble one another. The X-band EPR spectra recorded as frozen DMA solutions at 4 K are presented in Figure 4B. All three spectra have comparable features at *g*-values of 4.0 and 2.0, which correspond to complexes having $S = {}^3/_2$ states with axial symmetry. The virtually identical optical and EPR properties of [Co^{II}H$_2$**2**^{iPr}]$^-$, [Co^{II}H**1**^{iPr}]$^-$, and [Co^{II}**0**^{iPr}]$^-$ suggest that the three complexes have comparable electronic structures, which undoubtedly correlates with similar structures among their primary coordination spheres.

Electrochemical Properties of [Co^{II}H$_2$2**^{iPr}]$^-$, [Co^{II}H**1**^{iPr}]$^-$, and [Co^{II}**0**^{iPr}]$^-$.** Cyclic voltammetry (CV) was used to explore the redox properties of the three Co^{II} complexes in DMF. CV experiments on [Co^{II}**0**^{iPr}]$^-$ show a quasi-reversible process at $E_{1/2} = -252$ mV vs [Cp$_2$Fe]$^+$/[Cp$_2$Fe], which is assigned to the Co^{III}/Co^{II} couple. In contrast, the other complexes exhibited only irreversible oxidation processes, making it difficult to compare directly the redox properties within the series of Co(II) species. Nevertheless, the anodic potential (E_{pa}) for the
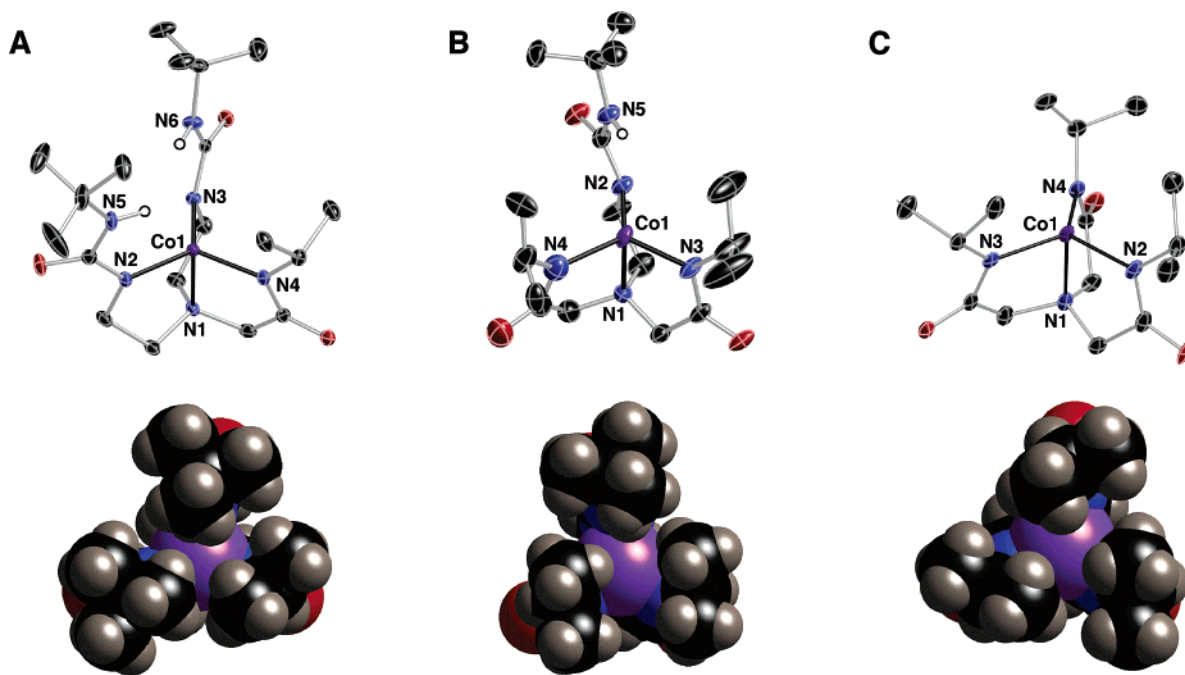
Figure 2. Thermal ellipsoid plots and space-filling representations of $[Co^{II}H_2\mathbf{2}^{iPr}]^-$ (A), $[Co^{II}H\mathbf{1}^{iPr}]^-$ (B), and $[Co^{II}\mathbf{0}^{iPr}]^-$ (C). Thermal ellipsoids are drawn at the 50% probability level, and only urea hydrogen atoms are depicted.
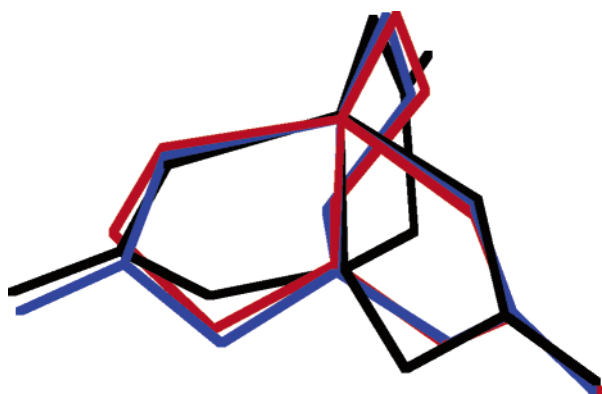
Figure 3. Overlap of the primary coordination spheres for $[Co^{II}H_2\mathbf{2}^{iPr}]^-$ (red), $[Co^{II}H\mathbf{1}^{iPr}]^-$ (blue), and $[Co^{II}\mathbf{0}^{iPr}]^-$ (black).

complexes scales linearly with the number of urea groups in the complex: $[Co^{II}H_2\mathbf{2}^{iPr}]^-$ (−385 mV), $[Co^{II}H\mathbf{1}^{iPr}]^-$ (−240 mV), and $[Co^{II}\mathbf{0}^{iPr}]^-$ (−155 mV). The trend in E_{pa} suggests that deprotonated ureas are more electron-donating than deprotonated amides, which is consistent with urea groups having higher pK_a values. However, this factor alone may not be the only contributor; the complexes' different secondary coordination spheres could also contribute to the observed differences in E_{pa}. It is known in metalloproteins that changes in the H-bond networks around metal centers influence redox potentials.[26] A similar effect could be occurring in $[Co^{II}H_2\mathbf{2}^{iPr}]^-$, $[Co^{II}H\mathbf{1}^{iPr}]^-$, and $[Co^{II}\mathbf{0}^{iPr}]^-$, which differ in the number of H-bond donors near

(25) For examples of other amidate ligand systems, see: Margerum, D. W. *Pure Appl. Chem.* **1983**, *55*, 23−34. (b) Collins, T. J. *Acc. Chem. Res.* **1994**, *27*, 279−285. (b) Collins, T. J. *Acc. Chem. Res.* **2002**, *35*, 782−790. (c) Collins, T. J.; Kostka, K. L.; Münck, E.; Uffelman, E. S. *J. Am. Chem. Soc.* **1990**, *112*, 5637−5639. (d) Collins, T. J.; Fox, B. G.; Hu, Z. G.; Kostka, K. L.; Münck, E.; Rickard, C. E. F.; Wright, L. J. *J. Am. Chem. Soc.* **1992**, *114*, 8724−8725. (e) Ghosh, A.; Tiago de Oliviera, F.; Yano, T.; Nishioka, T.; Beach, E. S.; Kinoshita, I.; Münck, E.; Ryabov, A. D.; Horwitz, C. P.; Collins, T. J. *J. Am. Chem. Soc.* **2005**, *127*, 2505−2513.
(26) Representative examples: (a) Vance, C. K.; Miller, A.-F. *Biochemistry* **2001**, *40*, 13079−13087. (b) Xie, J.; Yikilmaz, E.; Miller, A.-F.; Brunold, T. C. *J. Am. Chem. Soc.* **2002**, *124*, 3769−3774.

the cobalt centers. For instance, the oxidized Co(III) species would more likely bind additional ligands (i.e., solvent molecules), and the presence of intramolecular H-bond donors could assist this process, leading to lowering of the oxidation potentials.
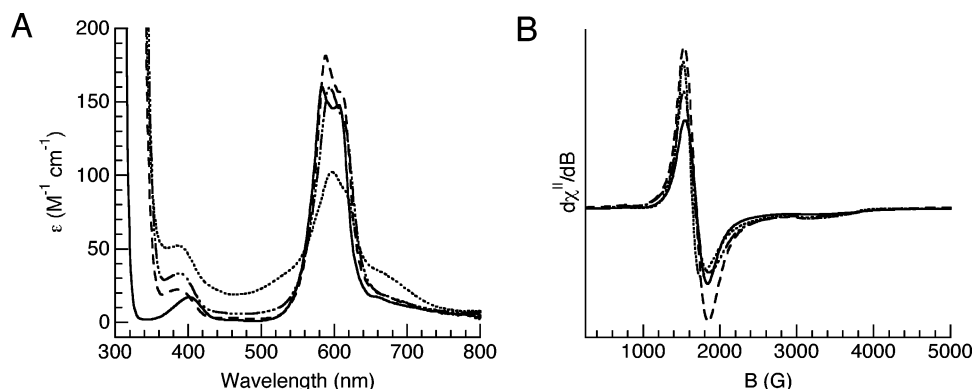
Properties of $[Co^{II}H_3buea]^-$. The synthesis of $[Co^{II}H_3buea]^-$ followed the same route as the other three Co(II) complexes. However, K$[Co^{II}H_3buea]$ cannot be redissolved after isolation, which has prevented further characterizations of this salt. In situ preparation of $[Co^{II}H_3buea]^-$ in DMA produces solutions that have properties resembling those of the other complexes. For instance, the absorbance spectrum of $[Co^{II}H_3buea]^-$ has features at the same wavelengths observed for other complexes, but with significantly lower molar absorbtivities values (Figure 4A). Moreover, the spectrum displays a broadness that is absent in the other three spectra, suggesting the possibility that more than one species may be present. The X-band EPR spectrum for $[Co^{II}H_3buea]^-$ generated in situ exhibits a broader axial signal with g-values consistent with an $S = \frac{3}{2}$ spin system (Figure 4B).

Reactivity with Dioxygen. $[Co^{II}H_3buea]^-$ and $[Co^{II}H_2\mathbf{2}^{iPr}]^-$. We have explored the reactivity profiles of the four cobalt(II) complexes with dioxygen. Spectroscopic and structural studies show that $[Co^{II}H_2\mathbf{2}^{iPr}]^-$, $[Co^{II}H\mathbf{1}^{iPr}]^-$, and $[Co^{II}\mathbf{0}^{iPr}]^-$ have similar primary coordination spheres, but differing in their cavity structures surrounding the coordinately unsaturated metal centers. Electrochemical results indicate some redox differences between the complexes, but the oxidation potentials for the three complexes are sufficiently negative so as to expect their ready reaction with dioxygen.[27] The data for $[Co^{II}H_3buea]^-$ give an uncertain picture of its structure(s) in solution, making direct comparisons with the other complexes difficult; however, we have included results of its reactivity toward dioxygen for completeness.

(27) Sawyer, D. T.; Sobkowiak, A.; Roberts, J. L., Jr. *Electrochemistry for Chemists*, 2nd ed.; Wiley-Interscience: New York, 1995; p 360.

Figure 4. Visible electron absorbance spectra measured in DMA at room temperature (A) and X-band EPR spectra of frozen DMA solutions recorded at 4 K (B): $[Co^{II}H_3\mathbf{3}^{iPr}]^-$ (•••), $[Co^{II}H_2\mathbf{2}^{iPr}]^-$ (— - - - —), $[Co^{II}H\mathbf{1}^{iPr}]^-$ (- - -), and $[Co^{II}\mathbf{0}^{iPr}]^-$ (—).

Scheme 4 ^{a}
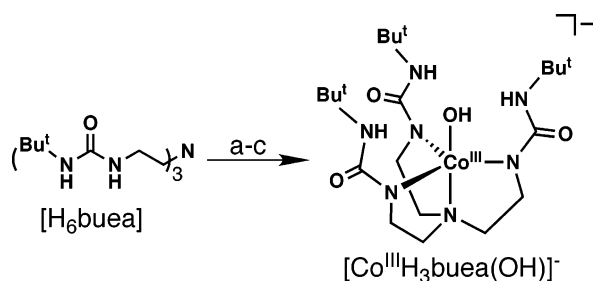
^{a} Conditions: (a) 3 KH, DMA, Ar, rt; (b) Co(OAc)$_2$, DMA, Ar, rt; (c) 0.5 equiv of O$_2$, DMA, rt.

Treating in situ prepared $[Co^{II}H_3buea]^-$ in DMA with 0.5 equiv of O$_2$ produced $[Co^{III}H_3buea(OH)]^-$ in 78% yield (Scheme 4). This complex has identical spectroscopic properties to those of $[Co^{III}H_3buea(OH)]^-$ prepared from oxidation of $[Co^{II}H_3buea-(OH)]^{2-}$, its Co^{II}–OH analogue. Confirmation that dioxygen was the source of the oxygen atom in the hydroxo ligand came from isotopic labeling studies. We synthesized $[Co^{III}H_3buea-(^{18}OH)]^-$ following the same procedure as that shown in Scheme 4 using $^{18}O_2$ as the oxidant. The solid-state FTIR spectrum of $[Co^{III}H_3buea(^{16}OH)]^-$ (Figure 5A) has a ν(O–H) band at 3589 cm^{-1} that shifts to 3579 cm^{-1} in $[Co^{III}H_3buea(^{18}OH)]^-$ ($\nu(^{16}OH)/\nu(^{18}OH) = 1.003$; calcd. 1.004). Another isotopically sensitive band observed at $\nu = 3621$ cm^{-1} in $[Co^{III}H_3buea(^{16}OH)]^-$ appears at $\nu = 3614$ cm^{-1} in the ^{18}O-isotopmer ($\nu(^{16}OH)/\nu(^{18}OH) = 1.002$).

Similar dioxygen reactivity was observed for $[Co^{II}H_2\mathbf{2}^{iPr}]^-$. Treating a DMA solution of $[Co^{II}H_2\mathbf{2}^{iPr}]^-$ with 0.55 equiv of O$_2$ afforded a red microcrystalline solid, whose analytical and spectroscopic properties are consistent with the formulation $[Co^{III}H_2\mathbf{2}^{iPr}(OH)]^-$ (eq 2). For example, this complex has a

$$(2)$$
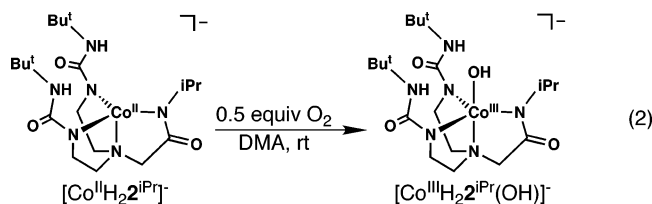
distinct FTIR peak at $\nu = 3661$ cm^{-1} assigned to the O–H stretch (Figure 5B). This band moves to the expected frequency ($\nu = 3650$ cm^{-1}) in $[Co^{III}H_2\mathbf{2}^{iPr}(^{18}OH)]^-$, again indicating that the O-atom of the hydroxo ligand is derived from dioxygen activation (vide supra). In comparison to the O–H vibration
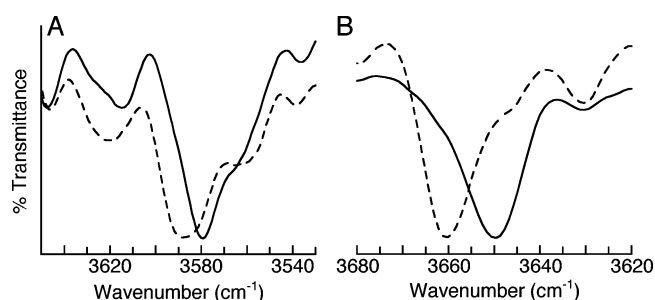
Figure 5. FTIR spectra of $[Co^{III}H_3buea(OH)]^-$ (A) and $[Co^{III}H_2\mathbf{2}^{iPr}(OH)]^-$ (B). Dashed-line spectra are complexes derived from $^{16}O_2$ and solid-lined are those from $^{18}O_2$.
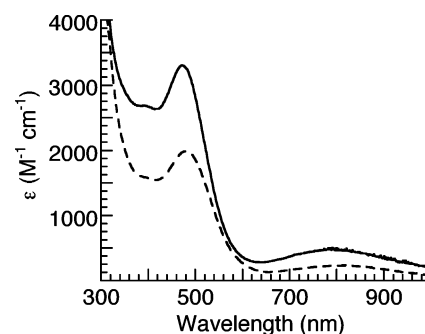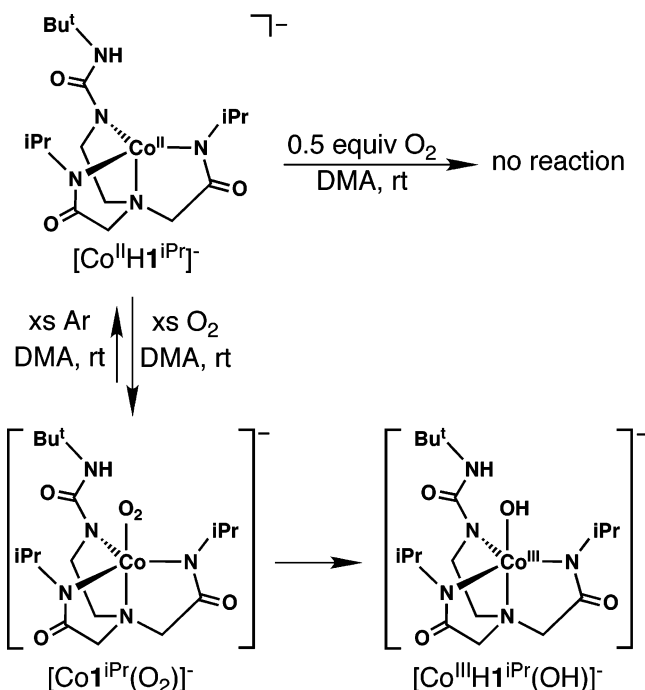

Figure 6. Visible electron absorbance spectra measured in DMA at room temperature for $[Co^{III}H_3buea(OH)]^-$ (—) and $[Co^{III}H_2\mathbf{2}^{iPr}(OH)]^-$ (- - -).

in $[Co^{III}H_3buea(OH)]^-$, the ν(O–H) in $[Co^{III}H_2\mathbf{2}^{iPr}(OH)]^-$ appears at a higher frequency, consistent with a reduced number of H-bond donors (and H-bonds) to the Co^{III}–OH unit. Note also that the visible absorbance features in $[Co^{III}H_2\mathbf{2}^{iPr}(OH)]^-$ are nearly identical to those found for $[Co^{III}H_3buea(OH)]^-$ (Figure 6).

The reaction of $[Co^{II}H_3buea]^-$ and $[Co^{II}H_2\mathbf{2}^{iPr}]^-$ with dioxygen provides rare examples of O$_2$ activation by Co^{II} species, for which reversible binding is the norm. Cobalt(II) complexes have been shown in a few examples to activate dioxygen; most of these are within the context of substrate oxidation processes in which the identity of the reactive cobalt species is unknown.[28] Several recent examples of dioxygen reactivity involving Co(I) complexes have been reported, including the characterization

(28) (a) Hanzlik, R. P.; Williamson, D. *J. Am. Chem. Soc.* **1976**, *98*, 6570–6573. (b) Sobkowiak, A.; Sawyer, D. T. *J. Am. Chem. Soc.* **1991**, *113*, 9520–9523. (c) Punniyamurthy, T.; Bhatia, B.; Reddy, M. M.; Maikap, G. C.; Iqbal, J. *Tetrahedron* **1997**, *53*, 7649–7670. (d) Jain, S. L.; Sain, D. *Angew. Chem., Int. Ed.* **2003**, *42*, 1265–1267.
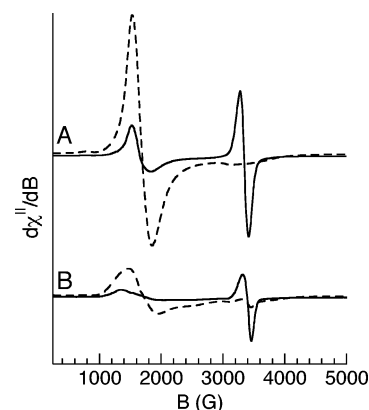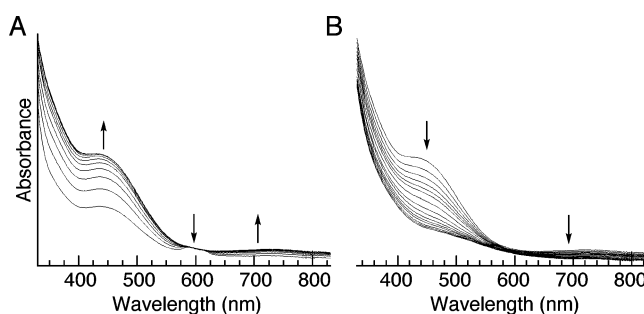
Scheme 5

Figure 7. X-band EPR spectra recorded at 4 K for [Co^{II}**H1**^{iPr}]$^-$ (- - -) and after treating with O$_2$ for 60 s (—) (A); after treating the oxygenated sample with argon (- - -) and after reintroducing O$_2$ for 60 s (—) (B). A 10 mM DMA solution of [Co^{II}**H1**^{iPr}]$^-$ was used.

Figure 8. Visible electron absorbance spectra for [Co^{II}**H1**^{iPr}]$^-$ after the addition of O$_2$ illustrating the production of [Co^{III}**H1**^{iPr}(OH)]$^-$ (A) and monitoring the change of [Co^{III}**H1**^{iPr}(OH)]$^-$ over time (B). Spectra in A and B were recorded at 1 and 25 min intervals, respectively.

of Co$-\eta^2-$O$_2$ adducts[29] as well as a dimeric Co$_2(\mu$-1,2-O$_2)_2$ species.[30] It is unclear if the reaction pathways leading to [Co^{III}H$_3$buea(OH)]$^-$ and [Co^{III}H$_2$**2**^{iPr}(OH)]$^-$ proceed through high valent intermediates with terminal oxo ligands, such as a Co$^{IV}-$oxo species;[31] related species have been proposed for dioxygen activation by iron and manganese complexes of the [H$_3$buea]$^{3-}$ ligand.[5b,i,j]

[Co^{II}H1^{iPr}]$^-$. The dioxygen reactivity of [Co^{II}**H1**^{iPr}]$^-$ is different than the other two Co(II) complexes. Under similar conditions used to prepare [Co^{III}H$_3$buea(OH)]$^-$ and [Co^{III}H$_2$**2**^{iPr}(OH)]$^-$, [Co^{II}**H1**^{iPr}]$^-$ does not appear to form a Co(III)$-$OH complex. Analysis of solutions prepared by treating a DMA solution of [Co^{II}**H1**^{iPr}]$^-$ with 0.5 equiv of O$_2$ shows that nearly all of the Co(II) starting compound is present (Scheme 5). Unreacted [Co^{II}**H1**^{iPr}]$^-$ remained even after its solution was stirred for 18 h, with no indication of oxidation.

The reaction was further investigated by bubbling an excess of dioxygen into solutions of [Co^{II}**H1**^{iPr}]$^-$ and analyzing for cobalt-containing species (Scheme 5). In one set of experiments, 10 mM DMA solutions of [Co^{II}**H1**^{iPr}]$^-$ in EPR tubes were treated with excess dioxygen for 1 min. After addition was completed, the samples were immediately frozen and analyzed by EPR spectroscopy at 4 K. The peak corresponding to [Co^{II}**H1**^{iPr}]$^-$ at $g = 4.0$ greatly diminished, and a new isotropic signal at $g = 2$ was observed (Figure 7A), suggesting a spin change to a species with an $S = \frac{1}{2}$ ground state. A Co$-$O$_2$

adduct, which is known to have $S = \frac{1}{2}$ ground states, is one possible species that could give rise to the $g = 2$ signal.[32] Revision to a spectrum that is similar to, but less intense, than that of [Co^{II}**H1**^{iPr}]$^-$ was accomplished by purging the sample with argon for 10 min (Figure 7B). Bubbling excess dioxygen into the thawed sample for 15 min reproduced the spectrum with the isotropic feature at $g = 2$ but at a lower intensity compared to the first cycle. These results are indicative of a system with some capability of reversible O$_2$ binding, which is known for Co(II) species.[33] However, the reversible process is lost over time as the species producing the $g = 2.0$ signal appears to have limited stability in DMA solution at room temperature. EPR spectra obtained periodically over the course of 24 h showed that the $g = 2.0$ signal diminished substantially, consistent with the results found for the O$_2$ cycling experiments shown in Figure 7.
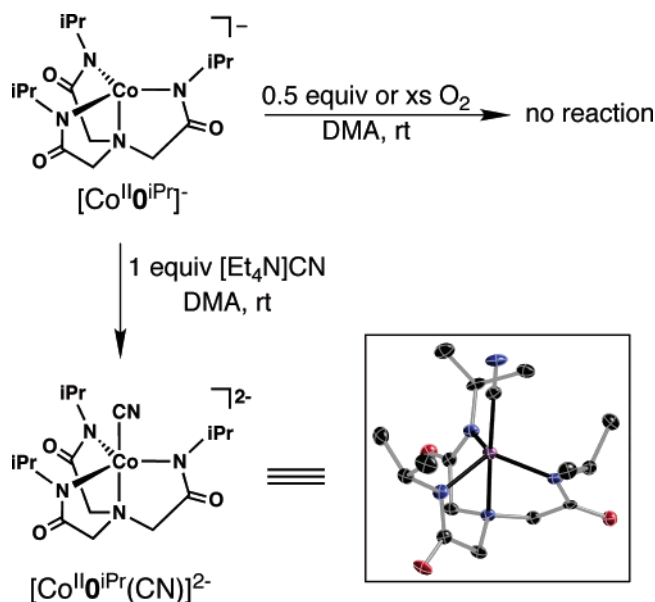
Monitoring the reaction with absorbance spectroscopy gave further insights into the dioxygen reactivity of [Co^{II}**H1**^{iPr}]$^-$. Figure 8A shows UV$-$vis spectra taken during the initial 30 min after treating [Co^{II}**H1**^{iPr}]$^-$ with excess dioxygen. The decrease in the bands at $\lambda_{max} = \sim$300 and 600 nm associated

(29) (a) Egan, J. W., Jr.; Haggerty, B. S.; Rheingold, A. L.; Sendlinger, S. C.; Theopold, K. H. *J. Am. Chem. Soc.* **1990**, *112*, 2445−2446. (b) Reinaud, O. M.; Theopold, K. H. *J. Am. Chem. Soc.* **1994**, *116*, 6979−6980. (c) Cramer, C. J.; Tolman, W. B.; Theopold, K. H.; Rheingold, A. L. *Proc. Natl. Acad. Sci. U.S.A.* **2003**, *100*, 3635−3640. (d) Hu, X.; Castro-Rodriguez, I.; Meyer, K. *J. Am. Chem. Soc.* **2004**, *126*, 13464−13473.
(30) Reinaud, O. M.; Yap, G. P. A.; Rheingold, A. L.; Theopold, K. H. *Angew, Chem., Int. Ed.* **1995**, *34*, 2051−2052.
(31) Cobalt(IV) species have been report; for examples, see: (a) Bower, B. K.; Tennent, H. G. *J. Am. Chem. Soc.* **1972**, *94*, 2512−2514. (b) Byrne, E. K. *J. Am. Chem. Soc.* **1987**, *109*, 1282−1283. (c) Vol'Pin, M. E.; Levitin, I. Y.; Sigan, A. L.; Nikitaev, A. T. *Organomet. Chem.* **1985**, *279*, 263−280. (d) Harmer, J.; Doorslaer, S. V.; Gromov, I.; Bröring, M.; Jeschke, G.; Schwieger, A. *J. Phys. Chem. B* **2002**, *106*, 2801−2811.

(32) (a) Basolo, F.; Hoffman, B. M.; Ibers, J. A. *Acc. Chem. Res.* **1975**, *8*, 384−392 and references therein. (b) Sharma, A.; Borovik, A. S. *J. Am. Chem. Soc.* **2000**, *122*, 8646−8655.
(33) (a) Jones, R. D.; Summerville, D. A.; Basolo, F. *Chem. Rev.* **1979**, *79*, 139−179 and references therein. (b) Niederhoffer, E. C.; Timmons, J. H.; Martell, A. E. *Chem. Rev.* **1984**, *84*, 137−203. (c) Norman, J. A.; Pez, G. P.; Roberts, D. A. In *Oxygen Complexes and Oxygen Activation by Transition Metal Metals*; Martell, A. E., Sawyer, D. T., Eds.; Plenum Press: New York, 1988; pp 107−127.

Scheme 6

$[Co^{II}\mathbf{0}^{iPr}]^-$

0.5 equiv or xs O_2
DMA, rt
⟶ no reaction

1 equiv [Et$_4$N]CN
DMA, rt

$[Co^{II}\mathbf{0}^{iPr}(CN)]^{2-}$

≡

with $[Co^{II}H\mathbf{1}^{iPr}]^-$ coincides with the appearance of new peaks at $\lambda_{max} = 430$ and 700 nm. The final optical spectrum in Figure 8A closely resembles those of the $Co^{III}-OH$ complexes $[Co^{III}H_2\mathbf{2}^{iPr}(OH)]^-$ and $[Co^{III}H_3buea(OH)]^-$ (Figure 6). Further support for the formulation of this species as a $Co^{III}-OH$ complex comes from FTIR studies on solid samples obtained via precipitation:[34] the spectra contain a signal at $\nu = 3633$ cm^{-1}, which is consistent with an O–H stretch. We have been unable to obtain this putative $[Co^{III}H\mathbf{1}^{iPr}(OH)]^-$ complex in pure form, which has prevented definitive characterization. Note that the $Co^{III}-OH$ complexes have a spin of $S = 1$ and thus are not detected in perpendicular-mode X-band EPR spectroscopy.

The observations just described provide some insights into a possible mechanism for the reaction between dioxygen and $[Co^{II}H\mathbf{1}]^-$ (Scheme 5). A $Co^{II}-O_2$ species is initially formed under conditions of excess dioxygen. While the $Co^{II}-O_2$ species is observable, it is relatively unstable and ultimately becomes a $Co^{III}-OH$ species, which we propose is $[Co^{III}H\mathbf{1}^{iPr}(OH)]^-$. The steps for this conversion are still not known. Moreover, this system is complicated by the instability of $[Co^{III}H\mathbf{1}^{iPr}(OH)]^-$, preventing us from obtaining it in pure form (vide infra).

$[Co^{II}\mathbf{0}^{iPr}]^-$. This Co(II) complex is unreactive toward dioxygen under our experimental conditions (Scheme 6). Treating $[Co^{II}\mathbf{0}^{iPr}]^-$ with 0.5 equiv of dioxygen or excess O_2 resulted in no observable change in its spectroscopic properties. Moreover, isolated samples after exposure to O_2 had properties identical to $[Co^{II}\mathbf{0}^{iPr}]^-$. The lack of dioxygen binding and reactivity is not attributed to steric effects caused by constraints within the secondary coordination sphere. We have previously found that Fe(II) and Mn(II) complexes of $[\mathbf{0}^{iPr}]^{3-}$ readily bind external ligands, including dioxygen.[11e] Furthermore, $[Co^{II}\mathbf{0}^{iPr}]^-$ binds a cyanide ion to form the five-coordinate Co(II)–cyano complex, $[Co^{II}\mathbf{0}^{iPr}(CN)]^{2-}$. The molecular structure of $[Co^{II}\mathbf{0}^{iPr}-(CN)]^{2-}$ determined by X-ray diffraction[35] is shown in Scheme

6 and confirms that the cyano ligand fits into the cavity formed by the three appended isopropyl groups.

Stability of the $Co^{III}-OH$ Complexes. We have also examined the stabilities of the three $Co^{III}-OH$ complexes in DMA at room temperature. As reported earlier, $[Co^{III}H_3buea(OH)]^-$ is stable for days in both the solid state and solution, showing no measurable loss of its signature absorbance features. In contrast, the other two $Co^{III}-OH$ complexes are less stable in solution: $[Co^{III}H_2\mathbf{2}^{iPr}(OH)]^-$ and $[Co^{III}H\mathbf{1}^{iPr}(OH)]^-$ decay with initial rate constants of 5.9×10^{-8} and 2.5×10^{-7} M min^{-1}, respectively.[36] The changes in the in situ generated $Co^{III}-OH$ complexes were observed spectrophotometrically, as shown in Figure 8B for $[Co^{III}H\mathbf{1}^{iPr}(OH)]^-$. The bands at $\lambda_{max} = 430$ and 700 nm that are indicative of $[Co^{III}H\mathbf{1}^{iPr}(OH)]^-$ diminish with no noticeable appearance of new features. A similar change was found for $[Co^{III}H_2\mathbf{2}^{iPr}(OH)]^-$. We have not yet determined the identity of the metal-containing species that results from these processes.

Effect of the Intramolecular H-Bonding Networks. The three well-characterized trigonal monopyramidal Co^{II} complexes $[Co^{II}H_2\mathbf{2}^{iPr}]^-$, $[Co^{II}H\mathbf{1}^{iPr}]^-$, and $[Co^{II}\mathbf{0}^{iPr}]^-$ have different levels of reactivity toward dioxygen, despite their nearly identical primary coordination spheres. As noted, there is a 0.23 V spread in the oxidation potentials between the complexes that would contribute to their observed reactions with O_2. The strongest reducing agent in the series, $[Co^{II}H_2\mathbf{2}^{iPr}]^-$, reacts readily with dioxygen to produce $[Co^{II}H_2\mathbf{2}^{iPr}(OH)]^-$ in good yield, even when using substoichiometric amounts of O_2. $[Co^{II}H\mathbf{1}^{iPr}]^-$ has an E_{pa} that is 0.145 V more positive yet only binds dioxygen when it is in excess. We have not observed dioxygen binding to $[Co^{II}\mathbf{0}^{iPr}]^-$ even though its E_{pa} is only 0.085 V more positive than that of $[Co^{II}H\mathbf{1}^{iPr}]^-$.

The difference in redox potentials cannot alone account for the observed O_2 chemistry in these Co^{II} complexes. We suggest that the addition of the intramolecular H-bond networks within the secondary coordination sphere assist in the binding of O_2 that leads to activation of dioxygen and formation of the $Co^{III}-OH$ complexes. The importance of H-bonds in dioxygen binding and activation is well documented in metalloproteins.[37] For instance, the removal of residues within the active sites that H-bond to the Fe–O_2 unit in hemoglobins causes a loss in respiration.[38] In addition, dioxygen affinity in hemoglobins has been correlated with the H-bond network surrounding the iron

(34) In a typical experiment, $[Co^{II}H\mathbf{1}^{iPr}]^-$ (0.29 mmol) in 3 mL of DMA was treated with excess dioxygen for 15 min, after which the reaction mixture was placed under reduced pressure for 5 min. The resulting heterogeneous mixture was filtered under argon, and the isolated solid was washed with diethyl ether and dried in vacuo to afford a tan powder.

(35) (Et$_4$N)$_2$[CoH$\mathbf{1}^{iPr}$(CN)] crystallized with one diethyl ether solvate per molecule in the triclinic space group $P2_1/n$ with the following cell constants: $a = 11.738(3)$ Å, $b = 31.298(8)$ Å, and $c = 12.271(4)$ Å; $\alpha = 90°$, $\beta = 116.695(5)°$, and $\gamma = 90°$; $V = 4038(2)$ Å^3, $Z = 4$; $R = 0.0783$, $R_w = 0.2064$ with a GOF(F^2) = 1.075. See Supporting Information for details.

(36) The initial rate constants for the decay of $[Co^{III}H_2\mathbf{2}^{iPr}(OH)]^-$ and $[Co^{III}H\mathbf{1}^{iPr}(OH)]^-$ were measured on solutions prepared with isolated complexes.

(37) Selected examples: (a) Holmes, M. A.; Stenkamp, R. E. *J. Mol. Biol.* **1991**, *220*, 723–737. (b) Fülöp, V.; Phizackerley, R. P.; Soltis, S. M.; Clifton, I. J.; Wakatuski, S.; Erman, J.; Hajdu, J.; Edwards, S. L. *Structure* **1994**, *2*, 201–208. (c) Mukai, M.; Nagano, S.; Tanaka, M.; Ishimori, K.; Morishima, I.; Ogura, T.; Watanabe, Y.; Kitagawa, T. *J. Am. Chem. Soc.* **1997**, *119*, 1758–1766 and references therein; (d) Dunietz, B. D.; Beachy, M. D.; Cao, Y.; Whittington, D. A.; Lippard, S. J.; Friesner, R. A. *J. Am. Chem. Soc.* **2000**, *122*, 2828–2839. (e) Gherman, B. F.; Dunietz, B. D.; Whittington, D. A.; Lippard, S. J.; Friesner, R. A. *J. Am. Chem. Soc.* **2001**, *123*, 3836–3837. (f) Du Bois, J.; Mizoguchi, T. J.; Lippard, S. J. *Coord. Chem. Rev.* **2000**, *200–202*, 443–485. (g) Berglund, G. I.; Carlsson, G. H.; Smith, A. T.; Szöke, H.; Henriksen, A.; Hajdu, J. *Nature* **2002**, *417*, 463–468. (h) Tomchick, D. R.; Phan, P.; Cymborowski, M.; Minor, W.; Holman, T. R. *Biochemistry* **2001**, *40*, 7509–7517.

(38) Perutz, M. F.; Fermi, G.; Luisi, B.; Shaanan, B.; Liddington, R. C. *Acc. Chem. Res.* **1987**, *20*, 309–321.

center.[39] Similarly, protein dysfunction is observed in cytochrome P450 when the active site H-bond network proximal to the $Fe-O_2$ moiety is disrupted.[40]

There is also a correlation between H-bonds and O_2 binding/activation observed by cobalt complexes described in this work. $[Co^{II}H_2 2^{iPr}]^-$ and $[Co^{II}H 1^{iPr}]^-$ are able to form intramolecular H-bonds in a $Co-O_2$ adduct; $[Co^{II}H_2 2^{iPr}]^-$, with two H-bond donors, clearly reacts at lower O_2 concentrations compared with $[Co^{II}H 1^{iPr}]^-$, which only has one H-bond donor. The additional H-bond donor in $[Co^{II}H_2 2^{iPr}]^-$ would assist in dioxygen binding, the essential first step in metal-mediated O_2 activation. Moreover, $[Co^{II} 0^{iPr}]^-$ does not bind dioxygen and is the only complex in the series that is incapable of forming intramolecular H-bonds.

Properties of the secondary coordination sphere also affect the stabilities of the $Co^{III}-OH$ complexes, which are the Co-based products isolated after dioxygen activation. In particular, the number of H-bond donors within the cavity correlates with the overall stabilities of these complexes. With its symmetrical cavity containing three H-bond donors, $[Co^{III}H_3buea(OH)]^-$ is stable for weeks in solution and can be crystallized, whereas $[Co^{III}H 1^{iPr}(OH)]^-$, with one H-bond donor, only has limited stability in solution. We propose that this effect is manifested in two synergistic ways. First, the greater number of H-bonds to the $Co^{III}-OH$ unit would reduce the nucleophility of the hydroxo ligand, rendering the complexes less likely to react with external species. Second, the greater number of intramolecular H-bonds would reinforce the cavity structure created by the urea groups, producing a more constrained microenvironment. The net result would be a more rigid cavity that limits access to the $Co^{III}-OH$ moiety.

Summary

We have described preparative routes to a new series of hybrid tripodal ligands. Convergent syntheses were developed having the potential to produce a variety of ligands containing at least one urea arm. In the present study, urea/carboxamide tripods were made in order to probe the effects of H-bonds on the binding and activation of dioxygen by cobalt(II) complexes. The hybrid ligands $[H_2 2^{iPr}]^{3-}$ and $[H 1^{iPr}]^{3-}$, along with the symmetrical carboxamide ligand $[0^{iPr}]^{3-}$, produce TMP Co(II) complexes with nearly identical primary coordination spheres and spectroscopic properties. In contrast, the complexes' secondary coordination spheres differ because of the varied structures formed around the cobalt ions by the tripodal ligands. The combination of urea and isopropyl groups produces cavities that place a different number of H-bond donors proximal to the cobalt centers. These systems illustrate our approach for producing site-specific modification of intramolecular H-bond networks, which permit investigations into the role of H-bonds in metal-mediated processes.

Our results strongly indicate that H-bond networks assist in the dioxygen binding/activation by synthetic cobalt(II) complexes. The importance of H-bonds in binding dioxygen to transition metal complexes has been recognized for years as a result of structural studies on myogoblin and hemoglobin variants.[4b,c,38,39] The cobalt complexes studied herein show that binding[4a] *and* activation are also affected by the numbers of H-bonds in the secondary sphere. The complexes with multiple H-bond donors readily bind and activate dioxygen. Thus, $[Co^{II}H_3buea]^-$ and $[Co^{II}H_2 2^{iPr}]^-$ react with substoichiometric amounts of dioxygen to produce $[Co^{III}H_3buea^{iPr}(OH)]^-$ and $[Co^{III}H_2 2^{iPr}(OH)]^-$, their corresponding $Co^{III}-OH$ derivatives, in $\sim 75\%$ yield. In contrast, $[Co^{II}H 1^{iPr}]^-$ only binds and reacts with dioxygen under saturating conditions, whereas $[Co^{II} 0^{iPr}]^-$, with no intramolecular H-bond donors, does not react with dioxygen. Moreover, there is a correlation between the number of intramolecular H-bonds and the stabilities of the $Co^{III}-OH$ complexes: the greater number of intramolecular H-bonds produces the more stable complex. These findings highlight the need to include secondary sphere effects in the design of transition metal complexes. Moreover, they illustrate how well-positioned H-bonds within the second sphere can impact metal-related chemistry.

Supporting Information Available: Cyclic voltammograms for the Co(II) complexes, data used for determining the initial rate constant for the decay of the $Co^{III}-OH$ complexes, and crystallographic details for $K[Co^{II}H_2 0^{iPr}]\cdot DMA$, $K[Co^{II}H 1^{iPr}]\cdot$ $0.5DMA\cdot 0.25Et_2O\cdot 0.25H_2O$, $K[Co^{II}H_2 2^{iPr}]\cdot Et_2O$, and $(Et_4N)_2$-$[CoH 1^{iPr}(CN)]\cdot Et_2O$. This material is available free of charge via the Internet at http://pubs.acs.org.

JA063935+

(39) (a) Kloek, A. P.; Yang, J.; Mathews, F. S.; Goldberg, D. E. *J. Biol. Chem.* **1993**, *268*, 17669−17671. (b) Yang, J.; Kloek, A. P.; Goldberg, D. E.; Mathews, F. S. *Proc. Natl. Acad. Sci. U.S.A.* **1995**, *92*, 4224−4228. (c) Huang, S.; Huang, J.; Kloek, A. P.; Goldberg, D. E.; Friedman, J. M. *J. Biol. Chem.* **1996**, *271*, 958−962.

(40) (a) Martinis, S. A.; Atkins, W. M.; Stayton, P. S.; Sligar, S. G. *J. Am. Chem. Soc.* **1989**, *111*, 9252−9253. (b) Gerber, N. C.; Sligar, S. G. *J. Am. Chem. Soc.* **1992**, *114*, 8742−8743. (c) Springer, B. A.; Sligar, S. G.; Olsen, J. S.; Philips, G. N., Jr. *Chem. Rev.* **1994**, *94*, 699−714. (d) Schlichting, I.; Berendzen, J.; Chu, K.; Stock, A. M.; Maves, S. A.; Benson, D. E.; Sweet, R. M.; Ringe, D.; Pestko, G. A.; Sligar, S. G. *Science* **2000**, *287*, 1615−1622.